CHANNEL ESTIMATION AND STATISTICAL ANALYSIS OF INDOOR ENVIRONMENT USING ULTRAWIDEBAND RADIO TECHNOLOGY

by

SHRUTHISHREE BANGALORE KRISHNAMURTHY

Presented to the Faculty of the Graduate School of

The University of Texas at Arlington in Partial Fulfillment

of the Requirements

for the Degree of

MASTER OF SCIENCE IN ELECTRICAL ENGINEERING

THE UNIVERSITY OF TEXAS AT ARLINGTON

August 2015

To Dear Mom, Dad and Sis

Acknowledgements

In an endeavor to successfully complete my thesis, I received assistance from many people and I take this opportunity to thank those who have helped me along the way to achieve this success.

I am grateful to my research advisor, Dr. Qilian Liang for his guidance and continuous support throughout my thesis. His patience and knowledge have been invaluable throughout my research and I express my deep sense of gratitude to him. I would like to thank Dr. Alan Davis and Dr. William Dillon for taking time to be on my thesis committee. I would like to thank my lab mates Sreevinay Netrapala, Karishma Katara and Roopesh Kumar Polaganga for their valuable suggestions during the course of my thesis.

I am indebted to my parents and my sister for always encouraging me and standing by my side. I would like to thank all my friends for their support and encouragement.

July 2, 2015

Abstract

CHANNEL ESTIMATION AND STATISTICAL ANALYSIS OF INDOOR ENVIRONMENT USING ULTRAWIDEBAND RADIO TECHNOLOGY

Shruthishree Bangalore Krishnamurthy, MS

The University of Texas at Arlington, 2015

Supervising Professor: Qilian Liang

Ultra-wideband technology finds various applications in radar technology, medical imaging, see-through-wall applications, surveillance and short distance communication applications. All of these applications require that the behavior of the channel be estimated giving a priori information about the various attributes of the channel like path loss, delay spread, channel capacity and so on. These parameters are the key to design an effective communication infrastructure suitable for the needs of the application.

In this thesis, the main aim was to model the channel and extract the various parameters related to the channel through data processing methods. In particular, a classroom environment was chosen and various scenarios were considered. Channel Impulse Responses (CIR) were extracted for the scenarios using the CLEAN algorithm, Empirical RMS delay spread and mean excess delay values were calculated from the CIR's. Values for path loss exponent and shadowing are also calculated. Based on the measurement data, the RMS delay spread and path loss have been modeled based on the probability density functions (PDFs) and the best distribution fits are provided. obtain the best distribution fits. The results obtained are compared with existing standards.

Table of Contents

List of Illustrations

List of Tables

Chapter 1

INTRODUCTION

1.1 Motivation

Ultra-wideband technology (UWB) is a radio technology used for transmission of information over a wide frequency band with a very low power spectral density allowing multiple users to access this wide range with no or negligible interference.

One of the major applications of this system is to replace the current technology high-data rate systems for short distances, as are, e.g., intended for wireless linking of home entertainment components (VCR, TV, Set-top boxes, etc.). A standard for such systems is currently being developed by the standardization group IEEE 802.15.3a. The target bitrates of this new standard are data rates of up to 110 Mbit/s at 10 m distance, 200 Mbit/s at 4 m distance, and higher data rates at smaller distances. More than 20 organizations have submitted proposals for this standard [1].

The objective of this work is to obtain a better assessment of the potentials of UWB indoor communications by characterizing the UWB indoor communication channel. Channel characterization refers to extracting the channel parameters from measured data. An indoor UWB measurement campaign is undertaken and time-domain indoor propagation measurements using pulses with a width of 61 pico-seconds (ps) are carried out. A classroom environment with various cases like Line of Sight (LOS) and Non Line of Sight (NLOS) are considered. Results for indoor propagation measurements are presented for large scale fading parameters and time dispersal parameters. The statistical analysis and simulation results of path-loss exponent (n) and time dispersion parameters are presented.

The primary hardware used for this study is PulsON 410 developed by The Time Domain Corporation. The focus of this thesis report is on channel modeling in a classroom environment and variation of RMS delay spread and path loss exponent values in different cases using PulsON 410 UWB radio in Bi-static mode. This radio also supports different types of software from Time Domain Corporation which plays a major role in conducting experiments.

1.2 Thesis Organization

This thesis is organized into six chapters. Chapter 1 introduces the current state of UWB technology with the importance of this piece of work. Chapter 2 gives a brief overview of ultra-wide band technology and its advantages over narrowband systems. Chapter 3 is about channel modeling in general and also the existing indoor model for UWB systems. Chapter 4 illustrates the equipment that was used to conduct the channel measurements and also explains the various parameters associated with the collected data. Chapter 5 presents the results of channel modeling in indoor classroom environment comprising of Channel Impulse Response's (CIR's), Power Delay Profile's (PDP's) and distribution fits for the small scale and large scale parameters. Chapter 6 summarizes the conclusions that are drawn from the results in chapter 5 and also discuss possible work to be done to extend the work presented in this thesis.

Chapter 2

ULTRA-WIDEBAND TECHNOLOGY

2.1 Introduction

In this chapter, an overview of the history behind development of ultra-wideband technology is presented followed by a brief introduction to various terminologies and advantages associated with it. Also, a discussion on the regulatory measures taken in order to prevent interference with existing narrowband systems is presented.

2.2 History of ultra-wideband

The history of ultra-wideband technology dates back to the early 1890's, in the spark gap transmission experiments performed by Marconi and Hertz. Thus, the very first wireless communication technique was based on the emission of short time domain pulses with very large bandwidth. Technological limitations however pushed the research towards the development of transmissions employing narrowband signals modulated with a carrier frequency typically some orders of magnitude larger than the signal bandwidth itself. Therefore, Shannon's pioneering work on the channel capacity, to make it potentially possible to achieve reliable and very high data rate transmission, even with extremely low Signal to Noise Ratio (SNR) if and only if a large signal bandwidth is used, found an obstacle in the practical realization of electronic components being able to properly work in large portions of the spectrum. It was only in the 1960s that baseband sub-nanosecond pulses found their applications for radar devices, due to their accurate spatial resolution, and because of the properties of low frequency components to penetrate objects. A few years later, in 1978, Bennet and Ross [2], when describing the applications of baseband radars, also proposed to use pulse techniques as the solution “to the problem of developing a short-range wireless communications link potentially providing the means for wireless transmission without licensing”. However, the advances in digital signal processing together with the increasing awareness of the radio spectrum as a limited resource, made most of the engineers skeptic towards pulse based wireless communication systems. From the end of 20th century the first related works of Win and Scholtz [3-6], which appeared contemporary to the rules of the Federal Communications Commissions (FCC) for ultra-wideband communications [7], gave a huge boost to this technology. In the first years of the new century, UWB was listed among the most impacting emerging communication technologies. In a handful of years, UWB gained the interest of both research and industry, as no other technology was able to do before. The unique potentials of UWB, with its premises to become a universal physical layer technique able to provide flexibility, high data rates, spectral efficiency, robustness towards interference, very low power transmission, accurate positioning capabilities, made this technology extremely attractive from a commercial point of view. The use of a bandwidth in the order of Giga Hertz and in the same order of magnitude as the central frequency, appeared as a problem with huge implications in the overall system model, design, and principle of operation. The very large fractional bandwidth required, led to reconsideration of traditional (narrowband or wideband) wireless channel models, since the different frequency components are affected in a significantly different way from the interaction with the propagation medium. Similar issues had to be addressed by antenna design engineers. From a system architecture point of view, the biggest challenge immediately appeared to be at the receiver side. On one hand, the huge signal bandwidth, allowing to resolve tens to hundreds of relevant multipath components, made the implementation of traditional rake receiver architectures extremely critical, not only for the number of branches required but also for the sub-nanosecond timing alignment needed for the replica in each branch. On the other hand, the maturity reached by digital signal processing techniques in traditional wireless communications could not be directly exploited due to the critical bottleneck of the analog to digital conversion step, which should be performed at several GHz rates to be able to rely on Nyquist based solutions. As a result of this, most of the big multinational companies immediately started to invest in a potentially impacting technology and several small and medium-sized enterprises focused on the development of wireless communication systems based on the impulse radio concept. Several thousands of scientific papers related to UWB communications and some dedicated conferences appeared in the academic world [19].

2.3 UWB Overview

The great difference between UWB and previous wireless technologies is first of all reflected in the unique peculiarities of its definition. In fact, the original distinguishing feature for the deployment of UWB radios was their potential ability to transmit in an unlicensed and very low power portion of the radio spectrum, allowing this technology to coexist with current and future licensed wireless systems. For this reason, the FCC does not directly specify any particular signal format or modulation technique for UWB; on the contrary, it strictly specifies the spectral and emission properties for this technology.

UWB is defined as any wireless system with bandwidth B ≥ 500 MHz, or a fractional bandwidth is given as

$$\text{Fractional Bandwidth} = \frac{f_H - f_L}{\frac{f_H + f_L}{2}} \geq 0.2, \qquad (2.1)$$

where f_H represents the upper frequency of the -10 dB emission limit and f_L represents the lower frequency limit of the -10dB emission limit [7]

For communication and positioning applications, the operating band is limited in the portion of the spectrum between 3.1 GHz and 10.6 GHz, provided that the emissions satisfy given limitations. These limitations have been defined with the pulse based ultra-wideband approach in mind, and distinguish between peak and average power:

- P_{meas}^{pk} ≤ 0 dBm in any 50 MHz signal bandwidth
- P_{meas}^{av} ≤ -41.3 dBm in any 1 MHz signal bandwidth

UWB is based on the generation of very short duration pulses of the order of picoseconds. The information of each bit in the binary sequence is transferred using one or more pulses by code repetition. The use of multiple pulses increases the robustness in the transmission of each bit. In UWB communications there is no carrier used and hence all the references are made with respect to the center frequency (f_c) [4].

$$\text{Center Frequency } (\mathrm{F}_c) = \frac{f_H + f_L}{2} \tag{2.2}$$

There are many advantages of UWB over conventional narrowband systems which makes it a desirable candidate for wireless communications. UWB provides a large instantaneous bandwidth that enables fine time resolution for network time distribution, precision location capability, or use as radar. It is characterized by short duration pulses that provide robust performance in dense multipath environments by exploiting more resolvable paths. Its low power spectral density allows coexistence with existing users and has a Low Probability of Intercept (LPI). Data rates may be traded for power spectral density and multipath performance [19].

2.4 Regulatory Issues

Since UWB signals usually occupy a very wide frequency band, it is inevitable that the UWB system has to share the already allocated frequency spectrum with other communications systems. Existing RF systems are concerned about the impact of UWB interference on their services. This led to the important regulatory standards of UWB technology.

In the United States, the FCC released its first authorization for UWB in February 2002 [8], which governed the use of UWB technology as a broadband wireless technology. The current FCC regulation for UWB is the Code of Federal Regulations (CFR), Title 47, Part 15, "Radio Frequency Devices" Subpart F for Ultra-Wideband Operation, published in June 2005 [9]. Specifically FCC allocated 7500 MHz of spectrum for unlicensed used of UWB devices in the 3.1GHz to 10.6 GHz frequency band. The FCC limits the Effective Isotropic Radiated Power (EIRP) to -41.3 dBm per MHz from 3.1GHz to 10.6 GHz for both indoor and handheld devices. Additional restrictions are placed on the radiated power outside of this band to minimize interference with Global Positioning Systems (GPS), aviation systems, and other sensitive communication systems. According to the above FCC regulations, it is likely that UWB technology will be initially used for short-range personal area networks in the tens of meters range. Thus, UWB will be competing with existing WLAN technologies like IEEE 802.11b, 802.11g, 802.11a, Bluetooth, and ETSI (European Telecommunications Standards Institute) Hiperlan/2. However, UWB is actually capable of longer distance transmission up to a few kilometers. But the FCC will require more studies and trials to be carried out before they consider the possibility of using UWB for extended range transmissions.

Note that the FCC does not specify the RF physical layer interface in the regulations but rather specify the spectrum requirements to balance the needs of the many licensed and unlicensed users. The RF physical layer interface is then defined through the standards community such as in the IEEE 802.15.3a standard for UWB communications, and industry groups like the Multi-Band OFDM Alliance (MBOA) [20].

Chapter 3

CHANNEL MODELLING

3.1 Introduction

The design of a wireless Transmitter and Receiver, the basic building blocks of any wireless infrastructure, is significantly dependent on the channel model corresponding to that communication scheme. The first step in understanding UWB channel measurements is that, we have two types: one is frequency domain measurement and the other is time domain measurement. In time domain measurement technique, the channel is excited with a pulse and the received signal is convolved with the pulse to obtain the channel impulse response. In frequency domain measurement technique, the frequency response of the channel is captured using a Vector Network Analyzer and the channel impulse response is extracted after applying Inverse Fast Fourier Transform. In either of the cases, the impact of the antenna on the measurements is crucial since the antenna characteristics vary significantly with the frequency, resulting in different responses in different directions [11].

Another crucial property of UWB is that each multipath component can show delay dispersion by itself. This means that a short pulse that undergoes only a single diffraction arrives at the receiver with a larger extent in delay domain compared to the originally transmitted pulse. The reason behind this is that the diffraction coefficient is frequency dependent. This now implies that the impulse response in a multipath environment is the sum of distorted, scaled and delayed pulses. The analysis and results from these findings led to classic ray-tracing approaches, resulting in a deterministic channel model for UWB [11].

On the contrary, statistical based characterization approaches immediately appeared more suitable to describe UWB indoor radio propagation in a more compact and easily interpretable way. The goal in this case is to give a representation of the essential properties of the UWB channel as a function of a set of random variables, without trying to replicate the exact behavior of the specific channel. The significant efforts, necessary to collect and characterize a large variety of propagation scenarios and conditions, resulted in the standardized IEEE models, which are currently commonly used as reference for algorithms simulation and performance evaluation.

3.2 The Time Domain Impulse Response model

Several channel models were proposed to characterize UWB channel propagation. Extensive measurement campaigns were undertaken in order to converge on a particular model. Finally, and IEEE task group was established in order to select a model that best approximates the channel behavior for UWB. In this regard, the standard proposed by IEEE was 802.15.3a which is based on the Saleh-Valenzuela (S-V) model, which describes that multipath components arrive in clusters. Also, the measurements were taken in time domain. The IEEE 802.15.3a standard was meant for high data rate application and for indoor environments. Subsequently, the committee developed another standard to support outdoor low data rate applications known as IEEE 802.13.4a [10, 11].

The S-V model states that the multipath components arrive in clusters and their amplitude follows a double exponential decay. On the contrary, results from UWB measurement campaigns led to a different conclusion in this aspect based on the fact that the multipath amplitude distribution followed a log-normal curve. Since this model was designed for baseband signaling, the phase of the channel impulse response was either 0 or π.

The received signal r(t) is expressed as follows:

$$r(t) = \sum_{n=1}^{N(t)} a_n(t) p(t - \tau_n(t)) + n(t) \tag{3.1}$$

where $a_{n(t)}$ and $\tau_n(t)$ are channel gain and delay measured at time t for the n -th path, $N(t)$ is the number of paths observed at time t and $n(t)$ is the additive noise at gains a_n , pulse arrival times τ_n and number of different paths N , which can be resolved at the receiver [10].

But this is not true when applied to IR since pulse shape modifications due to diffraction and penetration through different materials have not been accounted for. Thus, the shape of the pulse should be dependent on its propagation path and hence the received signal changes as given below:

$$r(t) = \sum_{n=1}^{N} a_n p(t - \tau_n) + n(t) \tag{3.2}$$

As suggested by Hashemi [12], it is more convenient to use the discrete time representation of the channel impulse response, where the time axis is represented in terms of bins. Bins are the smallest units of time where the receiver is incapable of observing more than one multipath component. The discrete impulse response of the channel is given by the following equation:

$$h(t) = \sum_{n=1}^{N_{\max}} a_n \delta(t - n\Delta\tau) \tag{3.3}$$

where $N_{\max}$ is the maximum number of bins considered within a single observation time interval, $\Delta\tau$ is the time duration of the bin.

3.3 Large scale parameters

In general, wireless multipath propagation can be characterized by two major effects according to the variability of power level, namely, large-scale fading and small scale fading. Large-scale fading can be categorized by the Path Loss (PL) and the shadowing. PL is an important characteristic for link budget calculation and system design which is defined as the ratio between the received and transmitted power.

The distance dependency of $PL(d)$, describes the attenuation of the median power as a function of distance traveled. The PL in dB as a function distance can be expressed as

$$PL(d) = PL_o + 10 \cdot n \cdot \log_{10}(\frac{d}{d_o}) + S; d \geq d_o \tag{3.4}$$

where $PL(d)$ represents the received power at a distance d, computed relative to a reference distance d_o, PL_o is the interception point and is usually calculated based on the mid-band frequency, n is the PL exponent and S is the shadowing fading parameter. The PL exponent is obtained by performing least squares linear regression on the logarithmic scatter plot of averaged received powers versus distance to Equation (3.4). [11]

The path loss observed at any given point will deviate from its average value [11]. This phenomenon is called shadowing and is defined as the slow variation of the local mean signal strength. The term “shadowing” is descriptive since typically these changes are due to the appearance or disappearance of shadowing objects on signal paths. It has been reported by many measurements in the literature to follow a log-normal distribution [13,14,15]. Referring to Equation (3.4), shadowing fading parameter is given by the term S that varies randomly from one location to another location within any home. It is a zero-mean Gaussian distributed random variables in dB with standard deviation σ_S which is also in dB. Different values of σ_S have been reported in the literature, ranging from 0.83 dB to 6 dB [16, 17], strongly depending on the measurement environments and scenarios.

3.4 Small scale parameters

According to the conventional S-V channel model [18] and the statistical-based UWB channel model proposed in [13, 15], the distributions of the cluster arrival times, T_l ,and the ray arrival times, $\tau_{k,l}$, are given by two Poisson processes. Thus, the cluster inter-arrival times and ray intra-arrival times are described by two independent exponential PDFs as follows:

$$p(T_l \mid T_{l-1}) = \Lambda \exp[-\Lambda(T_l - T_{l-1})] \quad 3.5)$$

$$p(\tau_{k,l} \mid \tau_{(k-1),l}) = \lambda \exp[-\lambda(\tau_{k,l} - \tau_{(k-1),l})] \quad (3.6)$$

where Λ is the mean cluster arrival rate and λ is the mean ray arrival rate. Typically, each cluster consists of many rays where $\lambda \gg \Lambda$. However, measurement results reported in [15] show that the single Poisson process given in Equation (3.6) is insufficient to model the ray arrival times in the indoor residential, indoor office, and outdoor office environments. Thus, mixtures of two Poisson processes is proposed in [13, 15] in order to model the ray arrival times

$$p(\tau_{k,l} \mid \tau_{(k-1),l}) = \beta\lambda_1 \exp[-\lambda_1(\tau_{k,l} - \tau_{(k-1),l})] \text{ (3.7)}$$

$$+(1-\beta)\lambda_2 \exp[-\lambda_2(\tau_{k,l} - \tau_{(k-1),l})], k > 0 \quad (3.7)$$

where β is the mixture probability, while λ_1 and λ_2 are the ray arrival rates. This new distribution gives an excellent match to the ray arrival times for the abovementioned three environments.

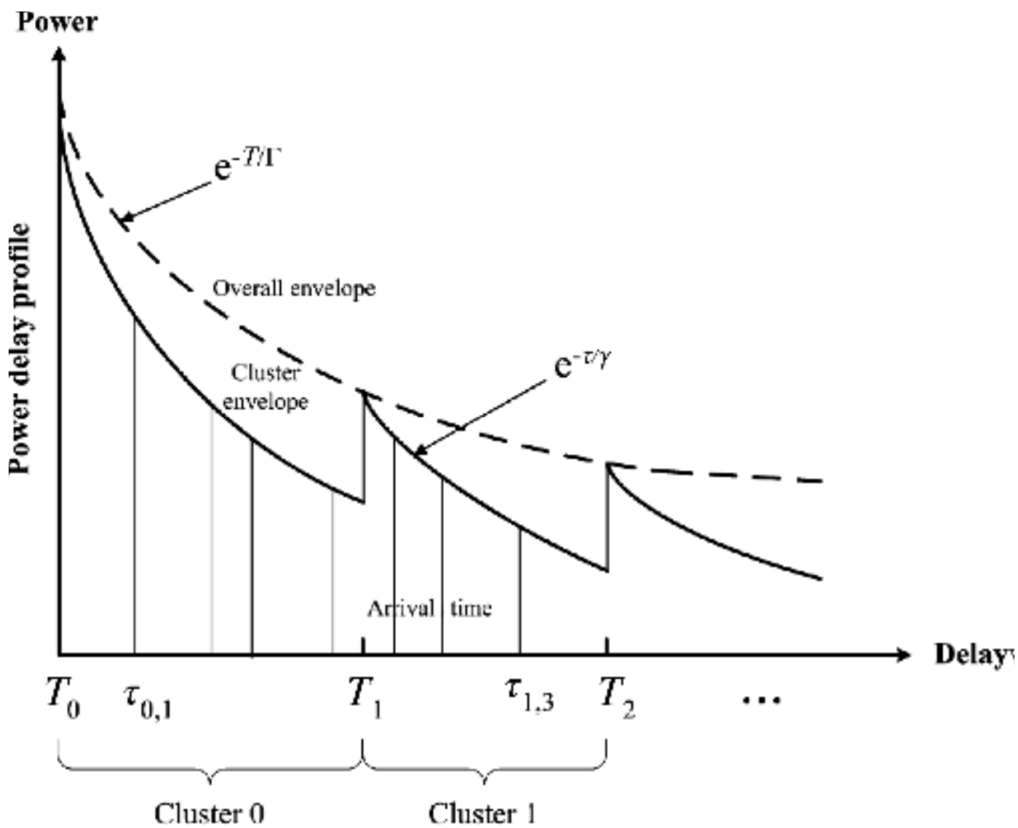

Figure 3-1 An illustration of the S-V channel model PDP with double exponential power decay phenomenon [11]

Figure 3-1 illustrates the typical power delay profile (PDP) of the S-V channel model with the double exponential power decay phenomenon. The cluster and ray decay time constants, Γ and γ, can be estimated from the measurement data by superimposing clusters and rays with normalized amplitudes and time delays and selecting their mean decay rates.

The mean excess delay is the weighted average of the power delay profile. It is the first moment of a PDP and is given by [11]

$$\bar{\tau} = \frac{\sum_i a_i^2 \tau_i}{\sum_i a_i^2} \tag{3.8}$$

where a_i^2 is the square of the amplitudes of the MPC and τ_i is the delay.

Root Mean Square delay spread (RMSDS) is the square root of the second central moment of a PDP and is given by,

$$\text{RMS delay spread} = \sqrt{\bar{\tau^2} - \bar{\tau}^2} \tag{3.9}$$

where $$\bar{\tau^2} = \frac{\sum_i a_i^2 \tau^2{}_i}{\sum_i a_i^2} \tag{3.10}$$

RMSDS is a measure of the multipath spread and it can be used to judge the performance of a communication system. It directly relates to inter-symbol interference. The larger the value of RMSDS, the greater the effect of inter-symbol interference.

Chapter 4

EQUIPMENT CONFIGURATION AND MEASUREMENTS

The hardware used for the experiments is PulsON 410. PulsON products have been developed by the Time Domain Corporation based on Time modulated Ultra Wideband (TM-UWB) architecture. The use of the PulsON radio in bi-static mode is explained in this chapter. Also some important terms associated with it is discussed. The waveform pulses are transmitted from a single omni-directional antenna and the scattered waveforms are received by another omni-directional antenna connected to another radio (bi-static nature). Any one of the two antenna ports on the P410 can be used for transmit and receive antennas

.

4.1 Using PlusON 410

The P410, shown in Figure 4.1, is a small, low power and affordable device which provides accurate, high rate range measurements and superior operational performance when compared to conventional RFID/RTLS devices [10].

Figure 4-1 P410 with Broad spec antenna from Time Domain Corporation [10]

Channel Analysis Tool (CAT) is a software tool that uses P400 or P410 platforms to view and log ultra wideband (UWB) RF waveforms as they propagate through an RF channel. These captured waveforms represent the impulse response of the environment. They can be used as a propagation tool to develop a channel model or as a bi-static radar[12].

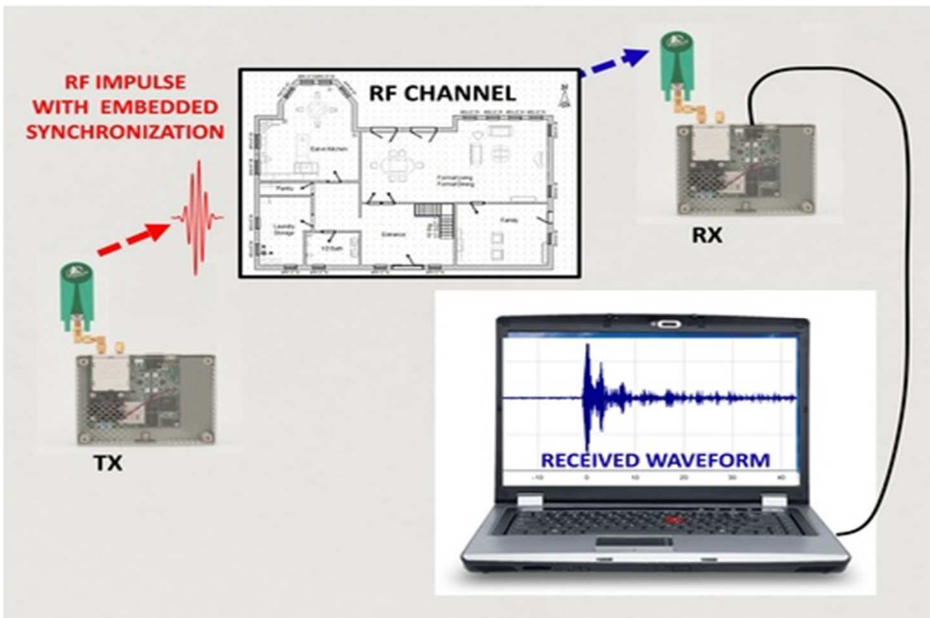

Figure 4-2 Block Diagram of P410 in CAT mode [12]

4.2 Key Features of the P410 in CAT mode

There are several key features of the PulsON radio listed below which makes it a suitable choice for conducting indoor propagation studies [11]

- Ideal for propagation studies
- No need for hardwired trigger signal between transmitter and receiver
- Lower cost and higher performance than DSO-based approaches

- Minimizes time required for propagation data collection campaigns
- Enables characterization of stationary and dynamic RF channels
- Allows user to analyze communications statistics of a UWB channel
- Can be used as a bi-static and multi-static radar
- UWB chipset enables small size and low power operation
- UWB waveform and pseudo random encoding ensures noise-like transmissions with a very small RF footprint
- RF transmissions from 3.1 GHz to 5.3 GHz, with center at 4.3 GHz

Provided below is the configuration that needs to be set through the GUI in the CAT application software. Successful connection to a radio brings up the configuration tab showing the device's current parameters. The parameters are divided into three general groupings: Commands, Parameter Settings, and Communications Statistics.

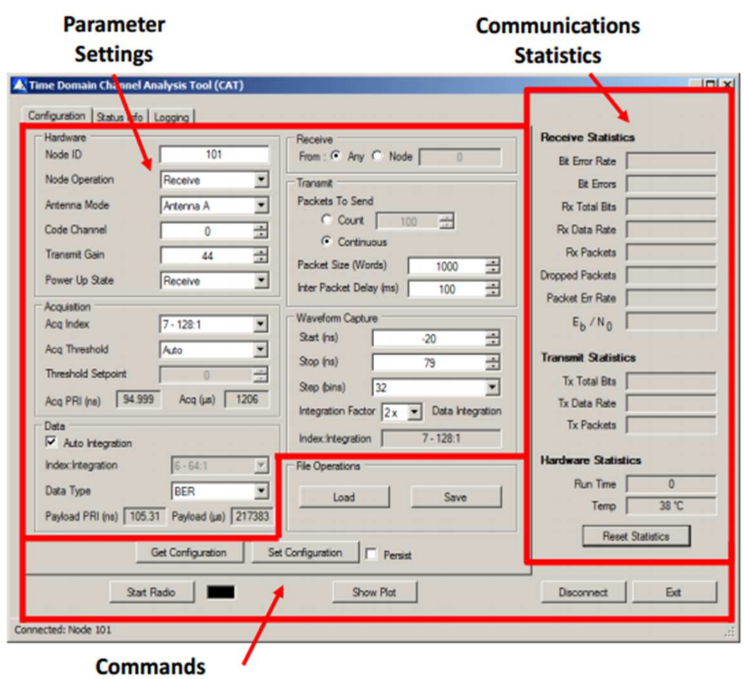

Figure 4-3 Configuration tab featuring set up tab

4.2.1 Acquisition Settings

These are the most important settings that need to be carefully reviewed before conducting an experiment. [12]

- **Acq Index:** Acquisition Pulse Integration Index (PII) determines the operating range at which transmissions can be acquired. The higher the value, the longer the operating range. Available values are 5 through 11.
- **Threshold:** This button has two values: Auto and Manual. If set to Auto, the Radio will determine the threshold for receiving signals. This is the preferred operating condition and the user should routinely use this setting.
- **Acq PRI (ns):** This is the Pulse Repetition Interval (PRI), measured in nanoseconds, between individual RF pulses transmitted in the acquisition portion of the transmitted packet. This parameter is a function of the selected Code Channel and typical has a value of approximately 100 ns.
- **Acq (µs):** This is the amount of time, in microseconds (µs), allocated for the packet acquisition header. It is a function of the selected Acq Index and Code Channel. This duration constitutes most, but not all, of the communications overhead.

4.2.2 Data Settings

- **Auto Integration:** This button determines if the data Index Integration (or data pulse integration index) will be determined automatically or by the user. If auto is selected, then CAT will automatically set the integration to one PII index value lower than the Acquisition Index. If Auto Integration is not set, then the user can selected a Data Index less than or equal to the Acq Index. This capability allows the user to reliably acquire packets but then send the data with lower integration, such that it reliably and repeatedly generates bit errors for determination of Bit Error Rate (BER) vs. Eb/No.

- **Index Integration:** This is the data Pulse Integration Index (PII) selected automatically by CAT or defined by the user.
- **Data Type:** This drop-down window determines if the data sent will be all ones, all zeros, or will be sent with a predefined pattern for computation of BER.
- **Payload PRI (ns):** This is the pulse repetition interval, measured in nanoseconds, between individual RF pulses transmitted in the payload portion of the RF packet. This parameter is a function of the selected Code Channel and typically has a value of approximately 100 ns.
- **Payload (µs):** This is the amount of time, in microseconds, allocated for the payload portion of the transmitted RF packet. It is a function of the selected Data Index: Integration (Data PII), the size of the data to be sent, and the Payload PRI.

4.2.3 Waveform Capture Settings

- **Start (ns):** The beginning point of a captured waveform in nanoseconds relative to the Radio lock spot. A negative value will start the waveform prior to the lock spot. A positive value starts the waveform after the lock spot. The maximum number of measurement points in a scan is 4094. When using a step size of 32 (one measurement every 61 ps), the user may select Start and Stop values between - 100 ns and +100 ns. For a step size of 64, the Start and Stop values can be between -200 ns to + 200 ns. Similarly, for step sizes smaller than 32, the Start and Stop values will be reduced by half each time the step size is reduced by half. The user should take care to ensure that the starting point is smaller/earlier than the ending point [12].
- **Stop (ns):** Stopping point of a captured waveform in nanoseconds relative to the Radio lock spot. Because of the manner in which the receiver works, the time

between the starting and stopping point will be in increments of 5.8 ns. The radio will round the user's stop point to reflect this limitation.

- **Step (bins):** This is the amount of time between measurements in a scan. A bin is approximately 1.9073 ps in duration. The standard amount of time between readings is 32 bins, or approximately 61.035 ps. This setting is rather coarse, but should be sufficient for most applications because the sampling rate is approximately twice the Nyquist rate. Alternate step sizes can be selected from the drop-down menu. It is important to note that the receiver architecture has been optimized to take waveform measurements at the 61 ps (32 bin) spacing. Selecting an alternate spacing will dramatically increase the amount of time necessary to collect a given scan. Selecting 64, 128, or 256 will reduce the rake efficiency by 50% and double the time required to collect a scan. Selecting any other value will reduce the rake efficiency by about 88% and thus increase the time required to collect a scan by a factor of 12.
- **Integration Factor :** This value defines the Pulse Integration Index (PII) to be used in collecting the waveforms. For a discussion of PII, see Appendix E. This value is shown as a factor of data integration. For example, if data integration is set to PII 6, and integration factor is set to 2x, then the waveform capture integration index will be set to PII 7.
- **Index Integration:** This field is computed by CAT and shows the waveform capture integration index selected by the user.

4.3 Experimental Setup

In this section, we will describe the experimental setup in detail for the various cases we have tested in the indoor Classroom Environment. These tests were conducted in Classroom 202 at Nedderman Hall, University of Texas at Arlington. In the following subsections we shall describe each case.

4.3.1 Case 1 / Scenario 1

Here both the TX and RX were placed at a height of 1m from the floor. During the experiment there were two people involved, each one next to TX and RX. The person sitting next to the TX was stationary and the other person was involved in moving the RX away from the TX in a horizontal direction. The RX is moved up to distance 12 m (length of the classroom) starting from a separation distance of 2 m. The LOS path in this case comprised of a large number of desks, benches and chairs below the level of sight of the antennae.

4.3.2 Case 2 / Scenario 2

Here both the TX and RX were placed at a height of 1 m from the floor. Two people were involved, each one next to TX and RX. The person sitting next to the TX was stationary and the other person was involved in moving the RX away from the TX in a Vertical direction. The RX is moved up to distance 10 m (length of the classroom) starting from a separation distance of 2 m. The LOS path in this case was relatively clear of clutter compared to case 1.

4.3.3 Case 3 / Scenario 3

Here also both the TX and RX were placed at a height of 1 m from the floor. During the experiment there were two people involved, each one next to TX and RX. Both the persons sitting next to the TX and RX were stationary and involved in operating the radios and logging waveforms. The TX and RX were separated by a distance of 7 m with a wooden board positioned midway between them. This is a NLOS case and also TX and RX are stationary / fixed.

4.3.4 Case 4 / Scenario 4

Here also both the TX and RX were placed at a height of 1 m from the floor. During the experiment there were two people involved, each one next to TX and RX. One person was involved to operate the TX and also act as an obstacle in between the TX and RX while the other person operated the RX and logged the raw data scans. The TX and RX were separated by a distance of 7 m (same as case 3) with the person stationary midway between them. This is a NLOS case and also TX and RX are fixed.

4.3.5 Case 5 / Scenario 5

Case 5 is very similar to case 4 in the context of distances and stationary nature of TX and RX. The only difference is that the human obstacle is non-stationary in this case moving from the TX towards the RX and back again for the duration of the experiment. This was tested to capture the differences that can be observed in the channel behavior with stationary and non-stationary clutter.

4.3.6 Case 6 / Scenario 6

Here both the TX and RX were placed at different heights. TX was at the ground level where as RX was at the far end of the classroom (10 m) at a height of approx. 3 m from the floor. During the experiment there were two people involved, each one next to TX and RX. One person was involved to operate the TX while the other person operated the RX and logged the raw data scans. This is a LOS case and also TX and RX are fixed.

Given below are some images of the classroom NH202 providing a better idea of the above scenarios.

Figure 4-4 Neddeman hall classroom NH 202 – front view

Figure 4-5 Nedderman hall classroom NH 202 – rear view

Chapter 5

RESULTS AND ANALYSIS

The results associated with each scenario in the classroom environment have been provided. In each scenario, approximately 500 snapshots of the channel data were taken into consideration for analysis to conclude and generalize the behavior of the channel. As illustrated previously, the CLEAN algorithm is used to extract the CIR data from the raw scans. Furthermore, Power Delay Profiles (PDP) was plotted for all the scenarios. RMS Delay spread (RMSDS) & Mean Excess Delay were estimated from PDP constituting the time dispersal parameters related to the small scale characteristics. In addition, path loss is also measured attributing to the large scale characteristics

5.1 Analysis of Small Scale parameters

RMS delay spread and Mean Excess Delay are two important small-scale parameters which helps us to characterize the channel as to the effective communication distance that can be achieved without any Inter Symbol Interference (ISI). In each scenario mentioned in the following sections, we have considered approximately 500 snapshots of channel data to extract CIR followed by their corresponding PDP's. The first central moment of the PDP characterizes the Mean Excess Delay whereas the Second central moment of the PDP characterizes the RMS Delay spread. In each snapshot comprising of 1632 samples, we have calculated the maximum and minimum values of RMS Delay spread. The minimum value is observed to be limited to a value of 0.5692 ns for all the scenarios. The maximum value is varying depending on the LOS and NLOS conditions. Although we have calculated the minimum and maximum values of RMS, the true value for a scenario is observed to be a simple average among all the snapshots for a particular case. Table 5.1 shows a comparison of the values between scenarios.

5.1.1 Scenario 1: Transmitter fixed / Receiver moving away in a Horizontal direction (LOS)

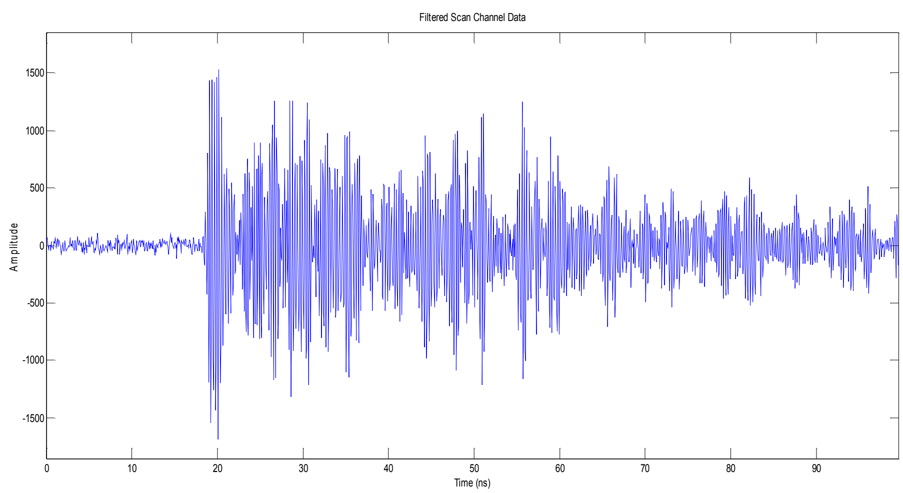

Figure 5-1 Filtered Scan Channel data – scenario 1

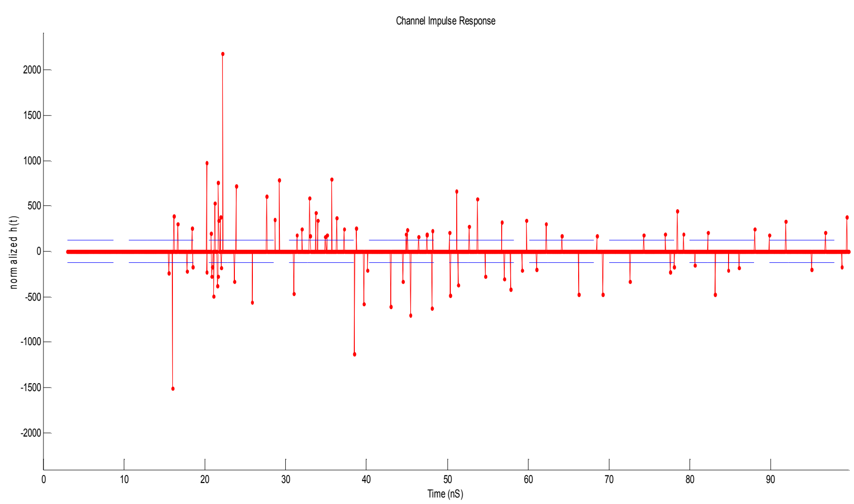

Figure 5-2 Channel Impulse Response – scenario 1

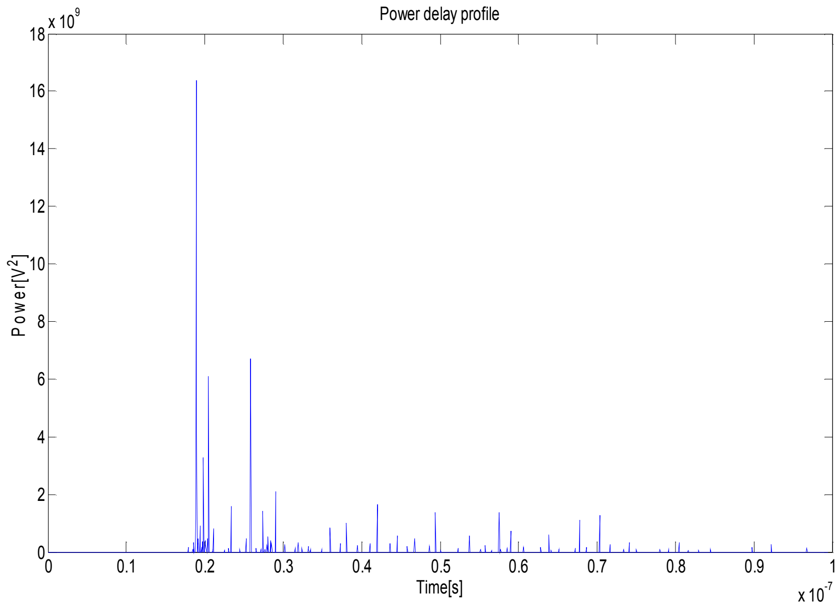

Figure 5-3 Power Delay Profile – scenario 1

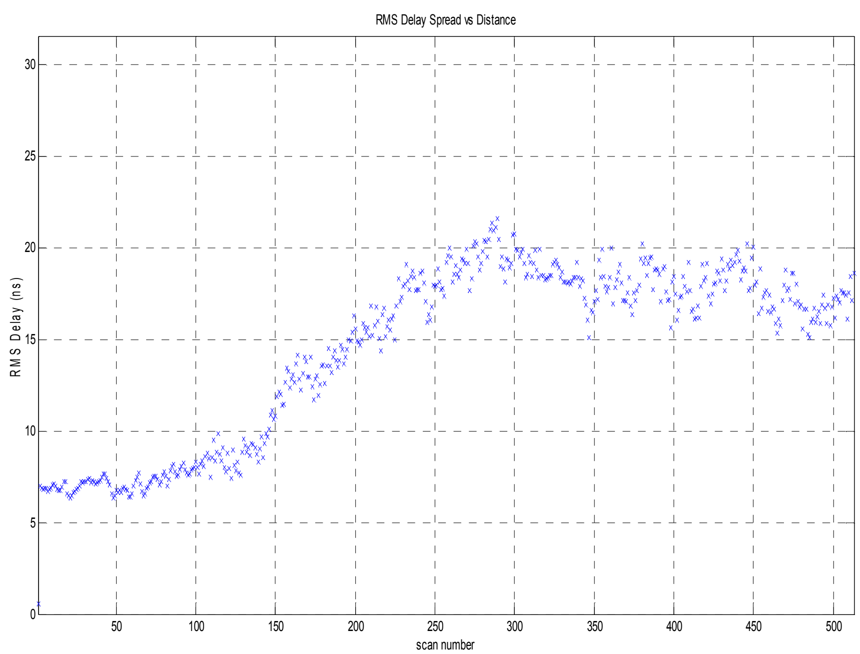

Figure 5-4 RMS Delay spread vs. Distance – scenario 1

5.1.2 Scenario 2: Transmitter fixed / Receiver moving away in a Vertical direction (LOS)

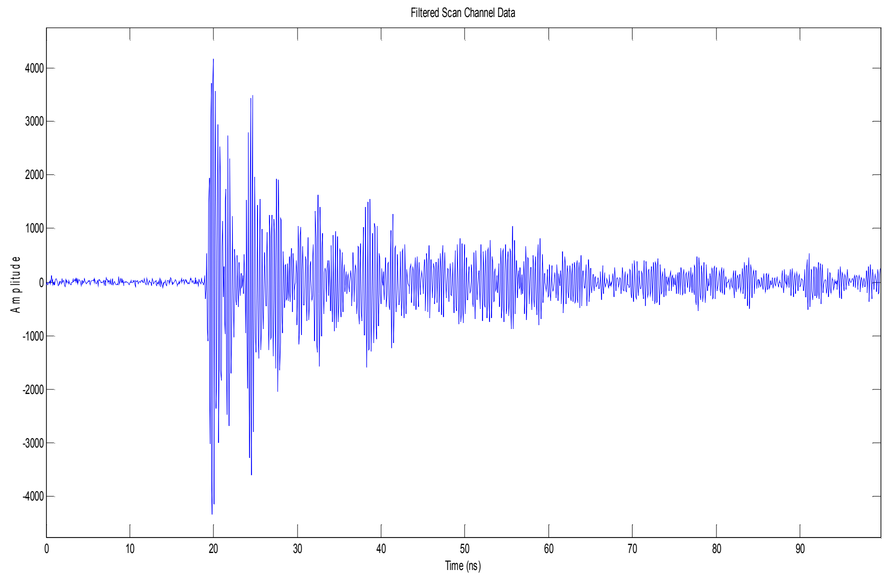

Figure 5-5 Filtered scan channel data – scenario 2

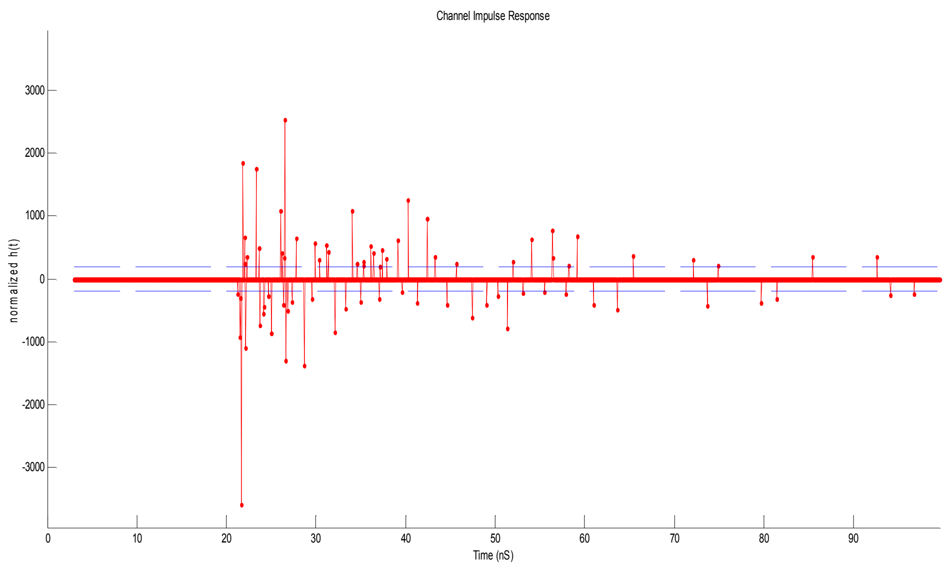

Figure 5-6 Channel Impulse Response – scenario 2

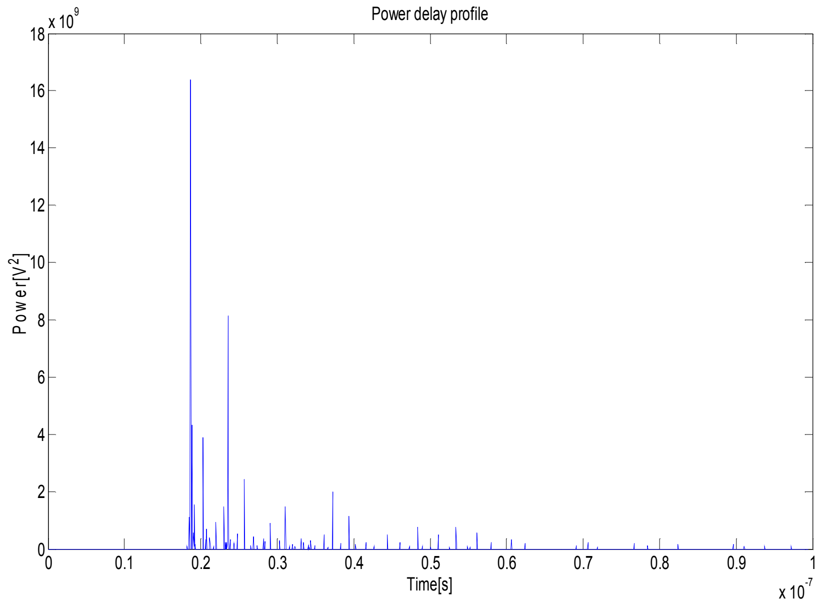

Figure 5-7 Power Delay Profile – scenario 2

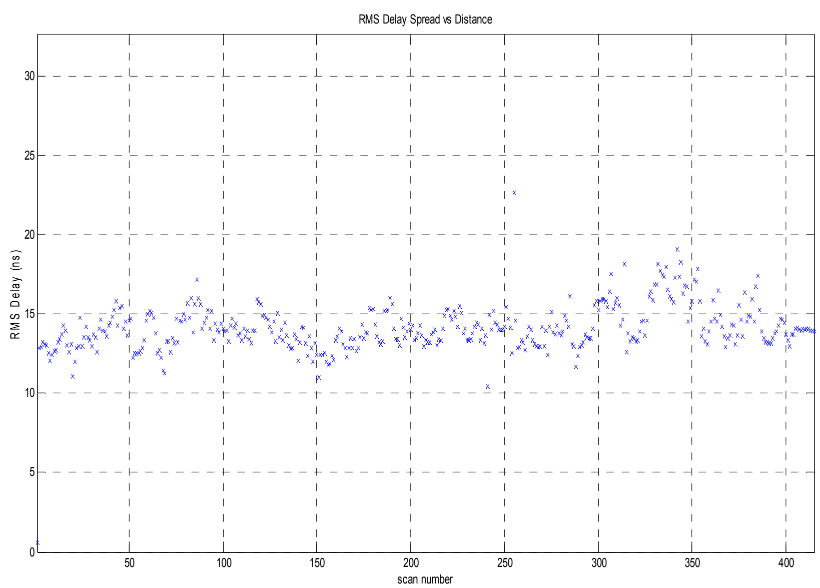

Figure 5-8 RMS Delay vs. Distance – scenario 2

5.1.3 *Scenario 3: Transmitter & Receiver / wooden board obstruction in between (NLOS)*

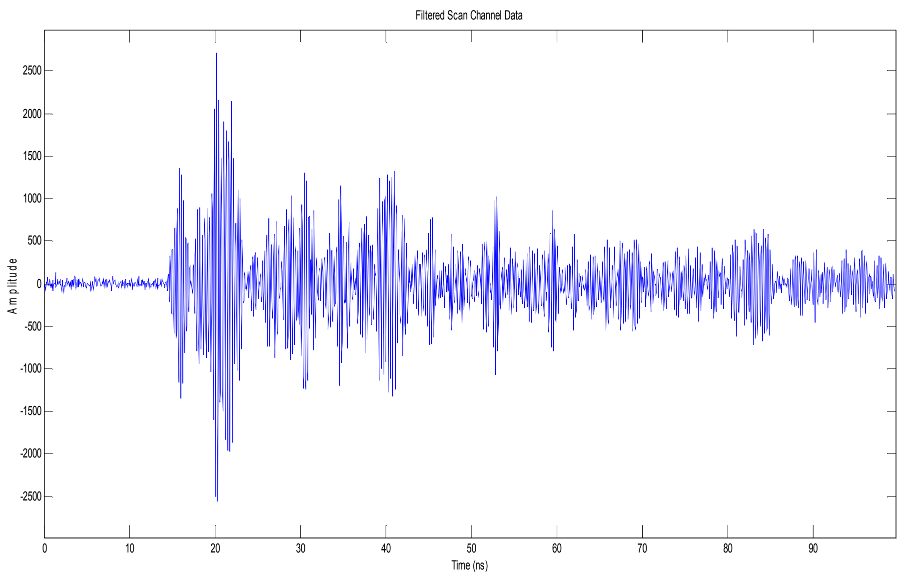

Figure 5-9 Filtered Scan Channel data – scenario 3

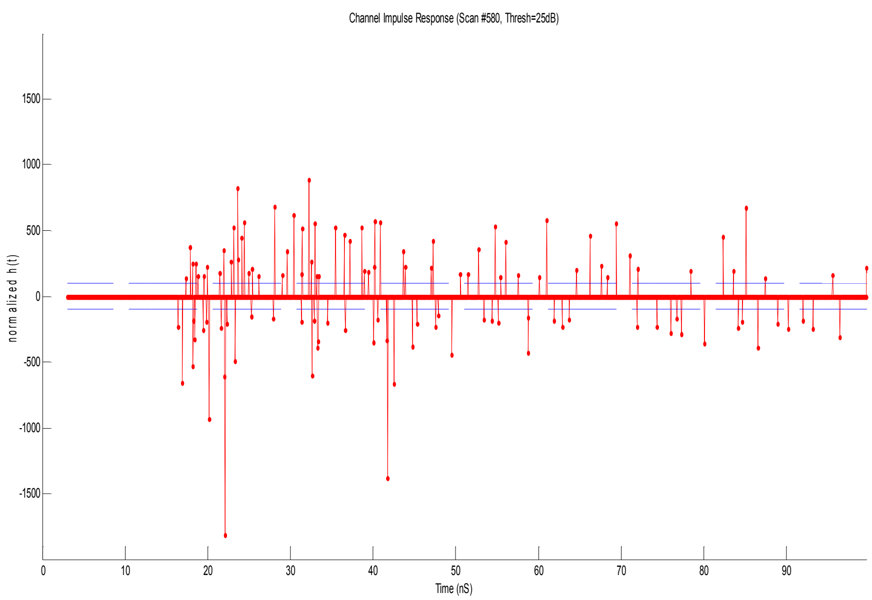

Figure 5-10 Channel Impulse Response – scenario 3

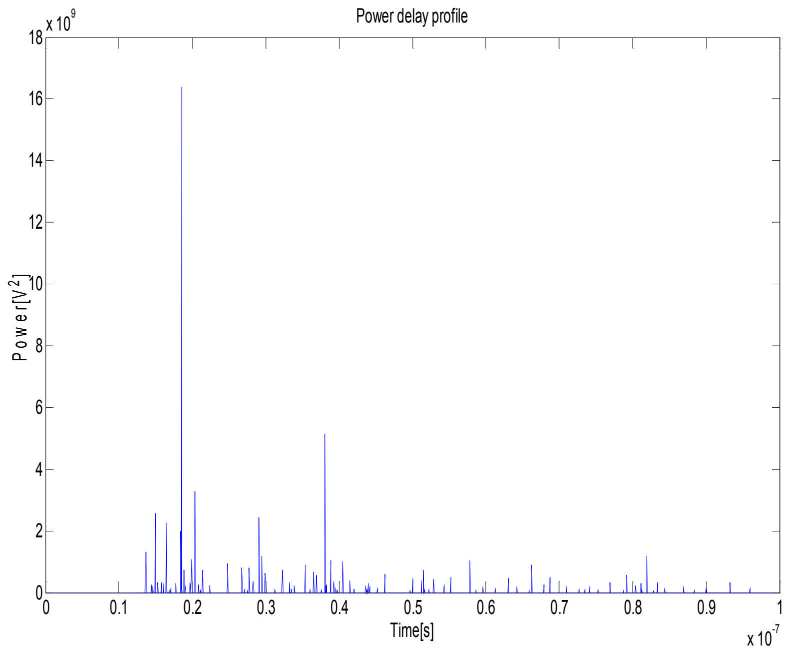

Figure 5-11 Power Delay Profile – scenario 3

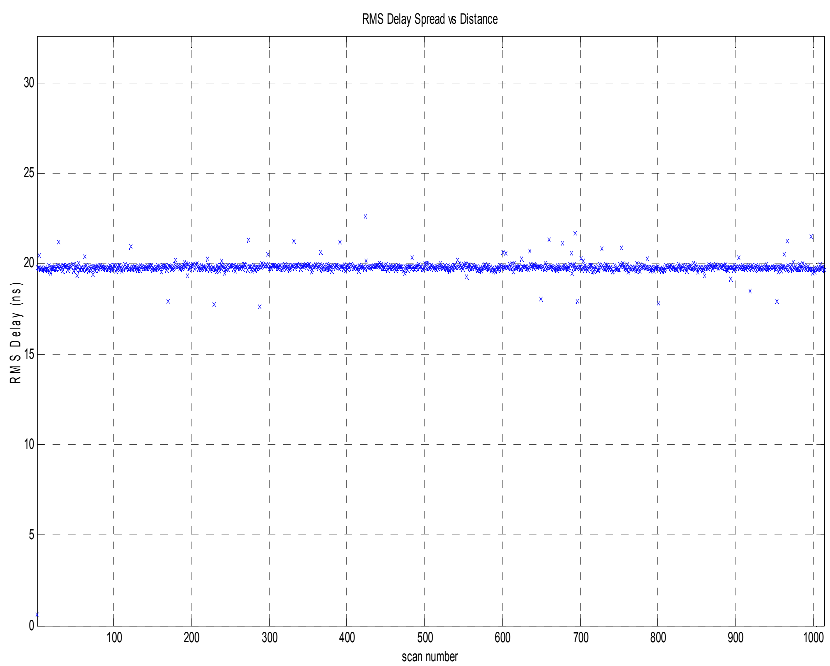

Figure 5-12 RMS Delay spread vs. Distance – scenario 3

5.1.4 Scenario 4: Transmitter and Receiver / Stationary Human in between (NLOS)

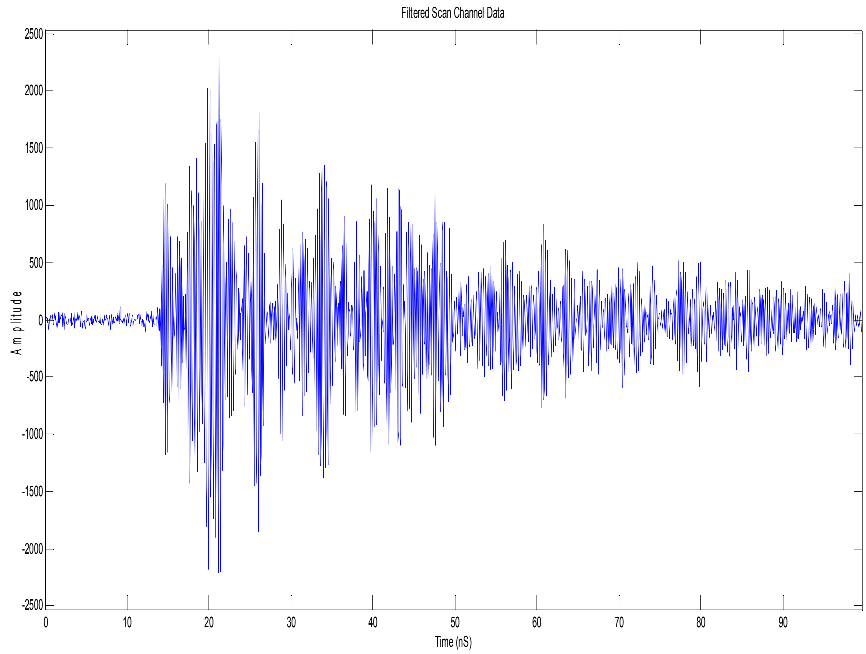

Figure 5-13 Filtered Scan Channel data – scenario 4

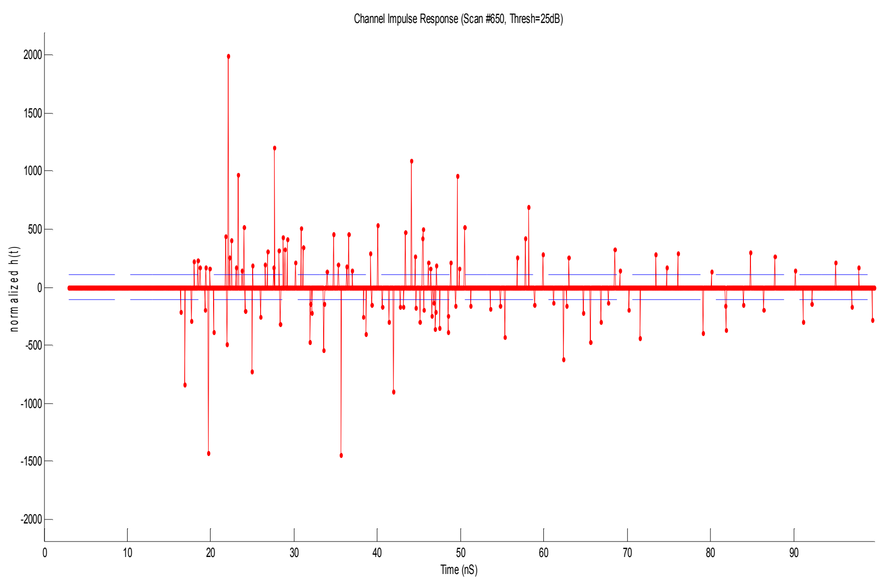

Figure 5-14 Channel Impulse Response – scenario 4

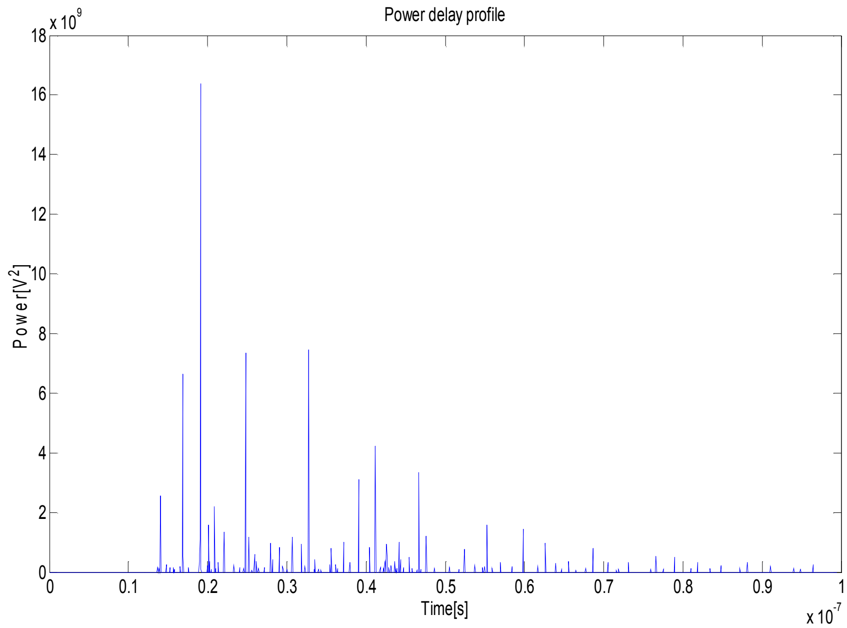

Figure 5-15 Power Delay Profile – scenario 4

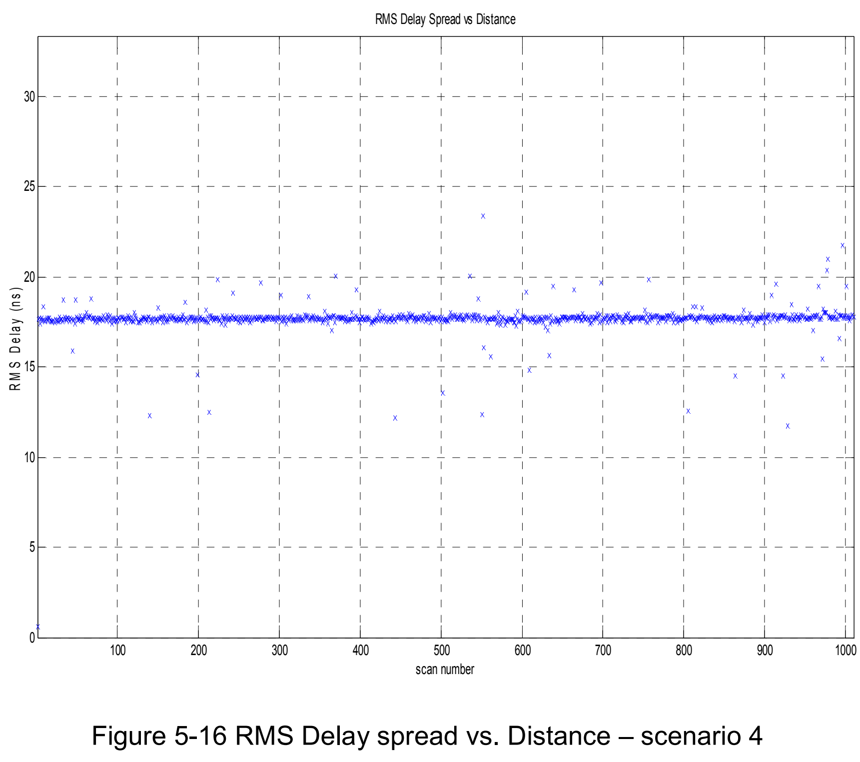

Figure 5-16 RMS Delay spread vs. Distance – scenario 4

<u>5.1.5 Scenario 5: Transmitter and Receiver / non-stationary Human obstacle (NLOS)</u>

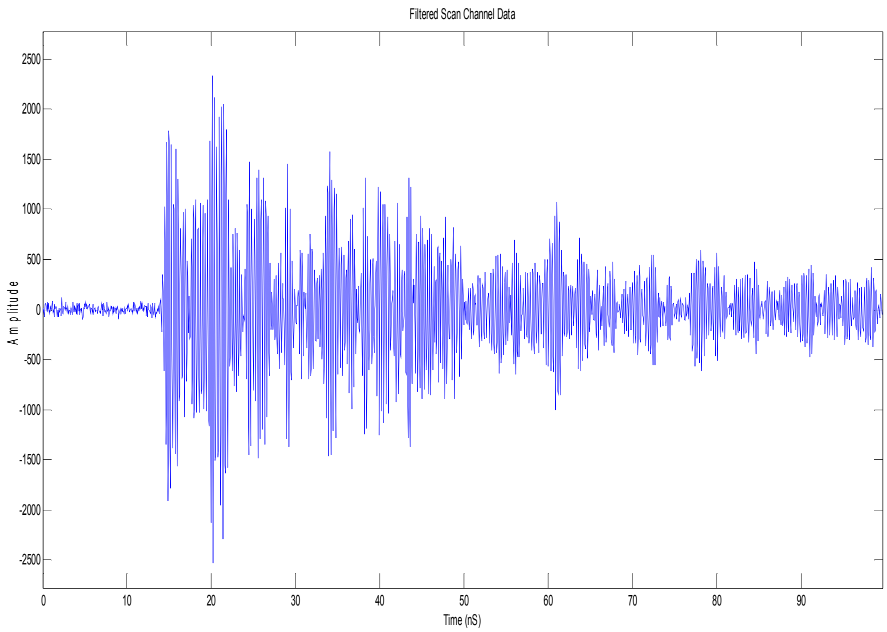

Figure 5-17 Filtered Scan channel data – scenario 5

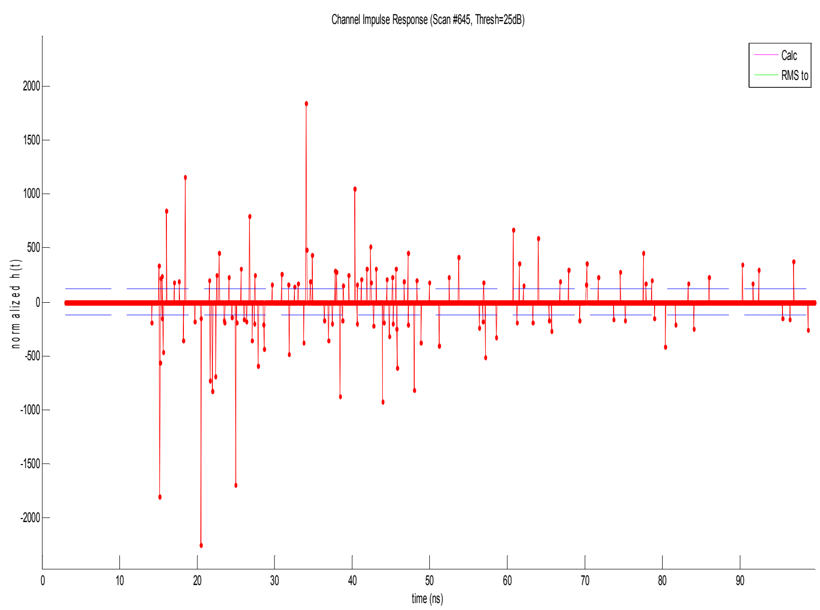

Figure 5-18 Channel Impulse Response – scenario 5

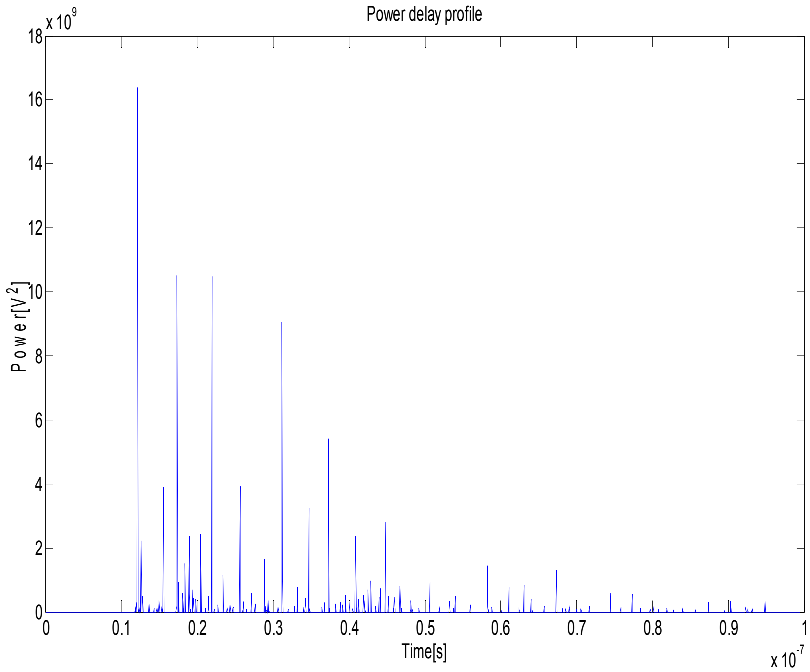

Figure 5-19 Power Delay Profile – scenario 5

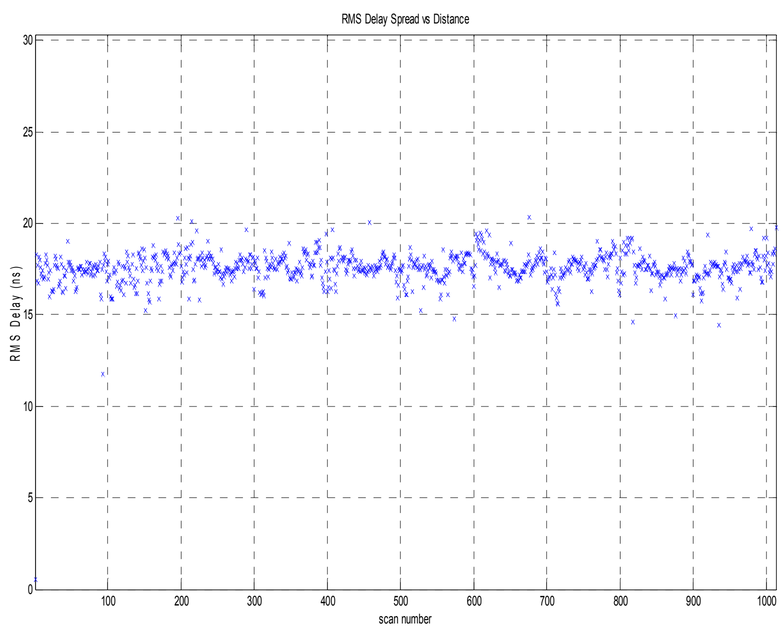

Figure 5-20 RMS Delay spread vs. Distance – scenario 5

5.1.6 Scenario 6: Transmitter and Receiver / Antennae are at different heights (LOS)

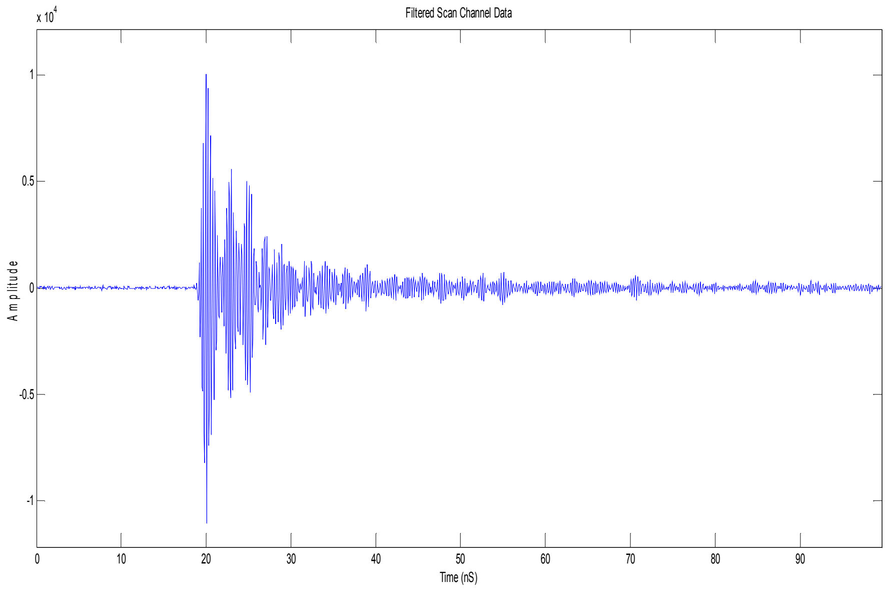

Figure 5-21 Filtered Scan Channel data – scenario 6

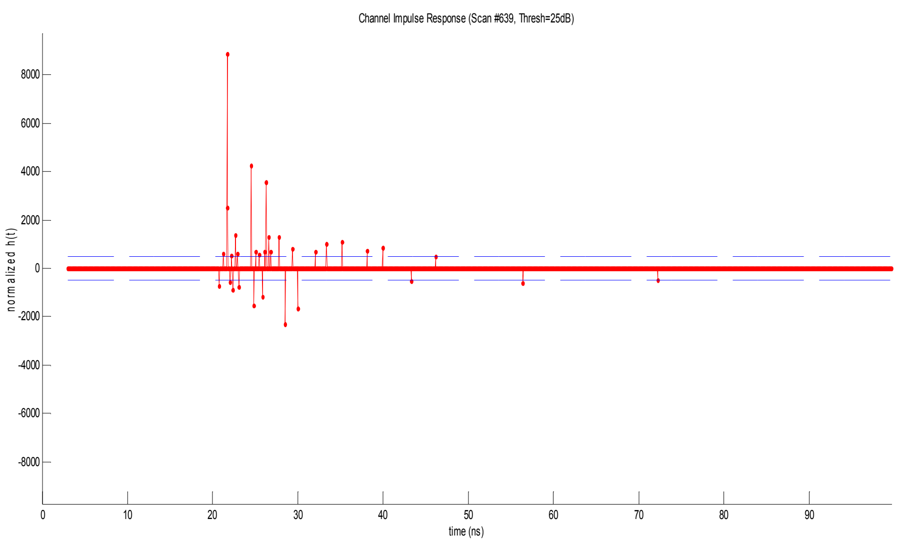

Figure 5-22 Channel Impulse Response – scenario 6

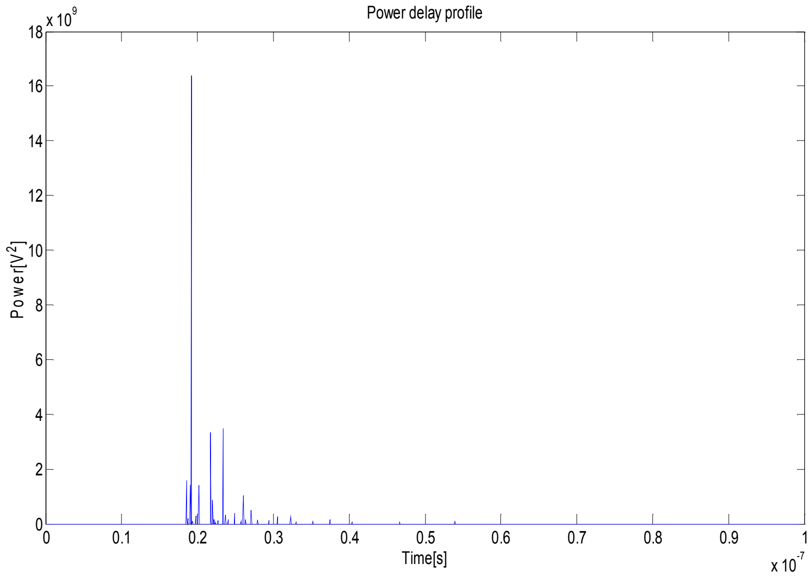

Figure 5-23 Power Delay Profile – scenario 6

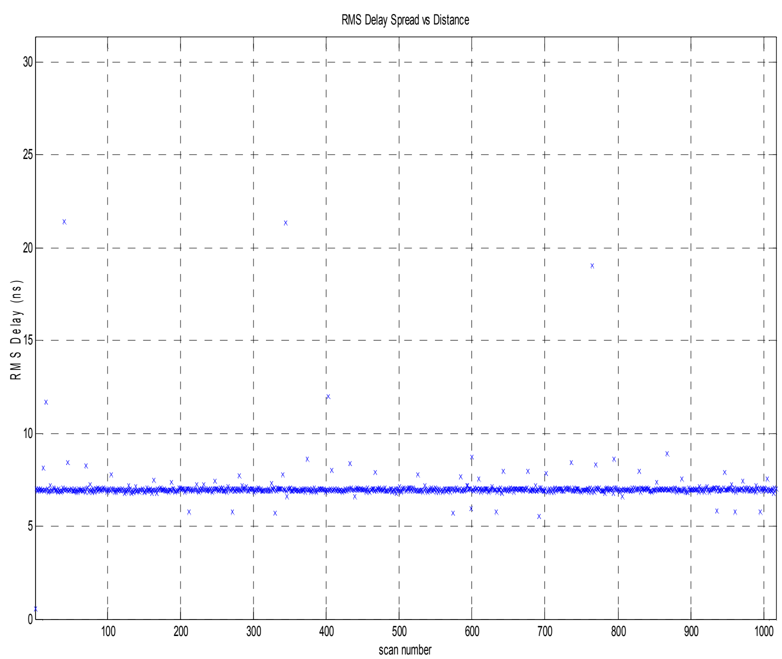

Figure 5-24 RMS Delay spread vs. Distance – scenario 6

5.1.7 Comparison of RMS Delay spread and Mean Excess Delay for all the scenarios

Provided below is Table 5-1 which compares the RMS values of the delay spread and mean excess delay of different cases in the classroom indoor environment. This comparison leads to several observations mentioned below:

1. The mean excess delay and RMS delay spread values in case LOS cases are less than that in the NLOS cases. This difference can be explained by recognizing in NLOS cases, the energy of the pulses fade due to excessive scattering and possible destructive interference caused by the obstruction between the transmitter and receiver
2. The maximum value of the RMS delay spread observed in all the scenarios is approximately in between 21 ns to 23 ns. The minimum value is bounded for all the cases and is never lower than 0.5692 ns.
3. The RMS delay spread in case of the wooden board as obstacle is larger than the human obstruction case. A possible explanation for this behavior would be based on the type of obstruction, dielectric constant or capacity of absorption of EM waves. Wooden board reflects more signal energy compared to The Human body.

Table 5-1 Comparison between different RMS delay spread and mean excess delay

Scenario	**Mean Excess Delay in ns**	**RMS Delay spread in ns (Average)**	**Max. RMS Delay spread in ns**	**Min. RMS Delay spread in ns**
TX and RX LOS (Classroom environment – Horizontal direction)	11.9553	14.4891	21.5702	0.5692
TX and RX LOS (Classroom environment – Vertical direction)	9.8088	14.1261	22.6962	0.5692
Wooden board obstacle b/w TX & RX (Classroom environment – NLOS)	21.2303	19.7788	22.5857	0.5692

Table 5-1 *(Continued)*

Stationary Human obstacle b/w TX & RX (Classroom environment – NLOS)	20.3729	17.6649	23.3412	0.5692
Non – stationary human obstacle b/w TX & RX (Classroom environment – NLOS)	18.7035	17.5895	20.3435	0.5692
TX & RX antenna at different heights (Classroom environment – LOS)	4.4608	7.0271	21.3882	0.5692

5.2 Comparison of Distribution fits for the different scenarios

5.2.1 Case 1: Transmitter Fixed / Receiver moving away in a horizontal direction (LOS)

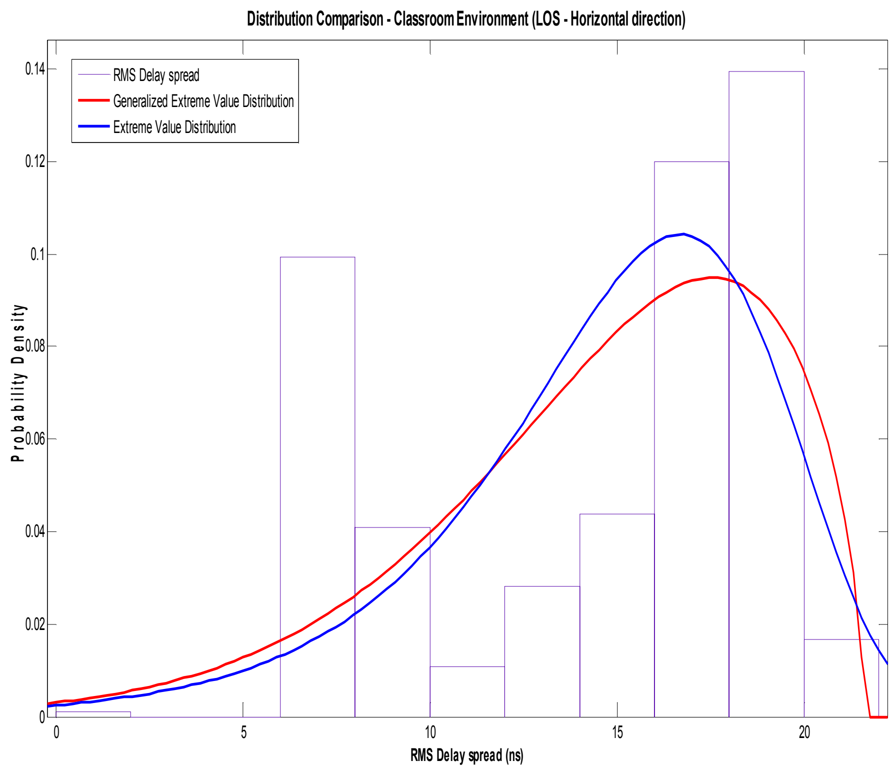

Figure 5-25 Distribution fitting of RMS Delay spread (Case 1)

Table 5-2 Comparison between Distributions for case 1

Distribution Type	Generalized Extreme Value	Extreme Value
Log Likelihood	-1453.93	-1479.4
Mean	14.4608	14.649
Variance	22.1345	20.4983

Table 5-3 Distribution parameters for GEV Distribution (case 1)

	Parameter Estimate	Standard Error
Mu	-0.645773	0.023225
Sigma	5.12262	0.19486
Nu	13.6635	0.239583

Table 5-4 Estimated covariance of parameter estimates GEV distribution (case 1)

	Mu	Sigma	Nu
Mu	0.000539402	-0.00296089	-0.0018336
Sigma	-0.00296089	0.0379705	-0.0228926
Nu	-0.0018336	-0.0228926	0.0574001

Table 5-5 Distribution parameters for Extreme Value Distribution (case 1)

	Parameter Estimate	Standard Error
Mu	16.6866	0.163556
Sigma	3.53008	0.131364

Table 5-6 Estimated covariance of parameter estimates of Extreme Value Distribution

(case 1)

	Mu	Sigma
Mu	0.0267504	-0.00651426
Sigma	-0.00651426	0.0172566

5.2.2 Case 2: Transmitter Fixed / Receiver moving away in a vertical direction (LOS)

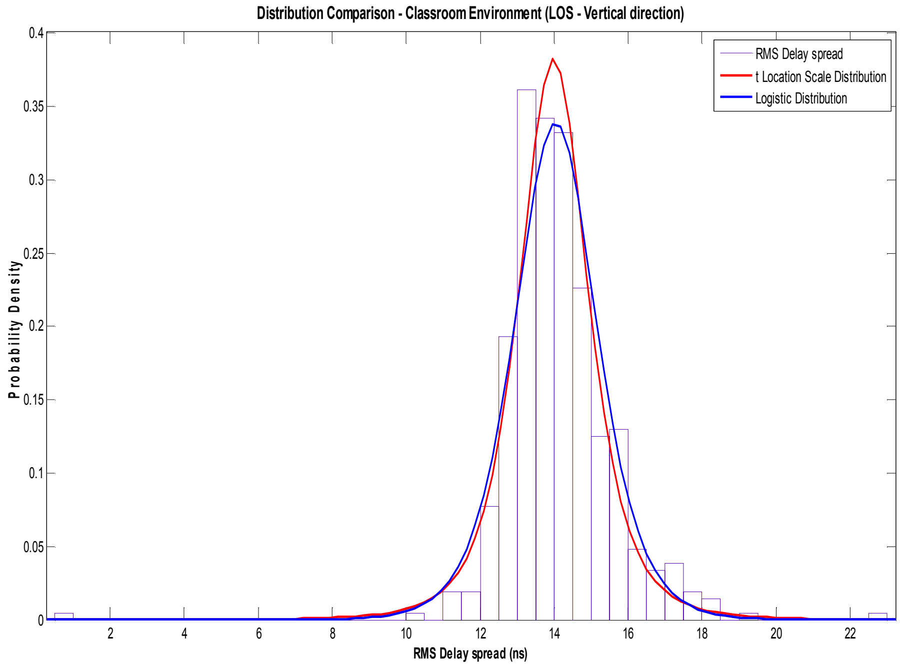

Figure 5-26 Distribution fitting of RMS Delay spread (Case 2)

Table 5-7 Comparison between Distributions for case 2

Distribution Type	T Location Scale	Logistic
Log Likelihood	-701.77	-712.813
Mean	13.9871	14.0432
Variance	2.1904	1.78878

Table 5-8 Distribution parameters for t Location Scale Distribution (case 2)

	Parameter Estimate	Standard Error
Mu	13.9871	0.0599951
Sigma	0.972067	0.0618378
Nu	3.51734	0.662634

Table 5-9 Estimated covariance of parameter estimates t Location scale distribution

(case 2)

	Mu	Sigma	Nu
Mu	0.00359941	0.000948812	0.010985
Sigma	0.000948812	0.00382392	0.0273441
Nu	0.010985	0.0273441	0.439084

Table 5-10 Distribution parameters for LOGISTIC Distribution (case 2)

	Parameter Estimate	Standard Error
Mu	14.0432	0.0618925
Sigma	0.737376	0.0306291

Table 5-11 Estimated covariance of parameter estimates of LOGISTIC Distribution

(case 2)

	Mu	Sigma
Mu	0.00383068	0.000106396
Sigma	0.000106396	0.000938142

5.2.3 Case 3: Transmitter & Receiver / wooden board obstruction in between (NLOS)

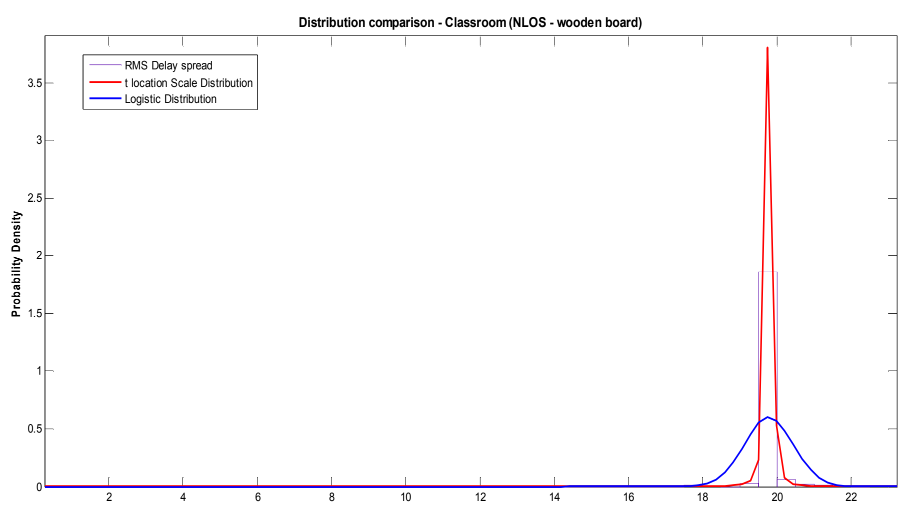

Figure 5-27 Distribution Fitting for RMS delay spread (Case 3)

Table 5-12 Comparison between distributions for case 3

Distribution Type	T Location Scale	Logistic
Log Likelihood	592.492	-1024.2
Mean	19.7888	19.7788
Variance	Inf	0.441852

Table 5-13 Distribution parameters for t Location Scale Distribution (case 3)

	Parameter Estimate	Standard Error
Mu	19.7888	0.0030839
Sigma	0.072837	0.00297874
Nu	1.76636	0.11955

Table 5-14 Estimated covariance of parameter estimates t Location scale distribution

(case 3)

	Mu	Sigma	Nu
Mu	9.51045e-06	-3.44474e-07	-1.29967e-05
Sigma	-3.44474e-07	8.87289e-06	0.00018016
Nu	-1.29967e-05	0.00018016	0.0142921

Table 5-15 Distribution parameters for LOGISTIC Distribution (case 3)

	Parameter Estimate	Standard Error
Mu	19.7788	0.0208747
Sigma	0.66472	0.0147716

Table 5-16 Estimated covariance of parameter estimates of LOGISTIC Distribution

(case 3)

	Mu	Sigma
Mu	0.000435752	4.68719e-19
Sigma	4.68719e-19	0.000218199

5.2.4 Case 4: Transmitter & Receiver / Stationary human obstruction between (NLOS)

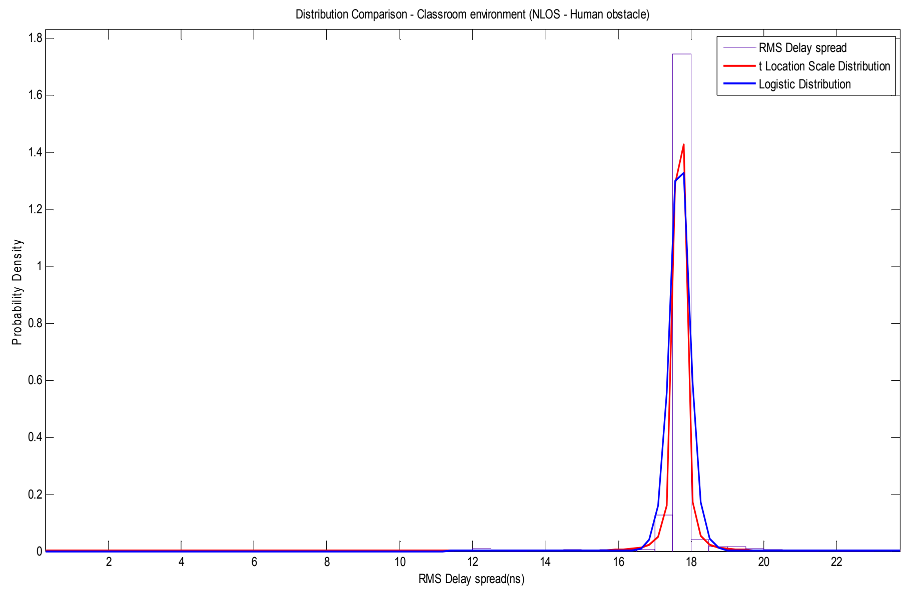

Figure 5-28 Distribution Fitting of RMS Delay spread (Case 4)

Table 5-17 Comparison between Distributions for case 4

Distribution Type	T Location Scale	Logistic
Log Likelihood	304.762	-438.52
Mean	17.6914	17.6928
Variance	Inf	0.0932636

Table 5-18 Distribution parameters for T Location Scale Distribution (case 4)

	Parameter Estimate	Standard Error
Mu	17.6914	0.00357415
Sigma	0.0804555	0.00347411
Nu	1.37592	0.0816594

Table 5-19 Estimated covariance of parameter estimates T Location scale distribution (case 4)

	Mu	Sigma	Nu
Mu	1.27745e-05	-2.34081e-07	-4.82007e-06
Sigma	-2.34081e-07	1.20695e-05	0.000134582
Nu	-4.82007e-06	0.000134582	0.00666826

Table 5-20 Distribution parameters for LOGISTIC Distribution (case 4)

	Parameter Estimate	Standard Error
Mu	17.6928	0.00810648
Sigma	0.168371	0.00489845

Table 5-21Estimated covariance of parameter estimates of LOGISTIC Distribution

(case 4)

	Mu	Sigma
Mu	6.57151e-05	4.8719e-07
Sigma	4.8719e-07	2.39948e-05

5.2.5 Case 5: Non Stationary human obstacle between Transmitter and Receiver (NLOS)

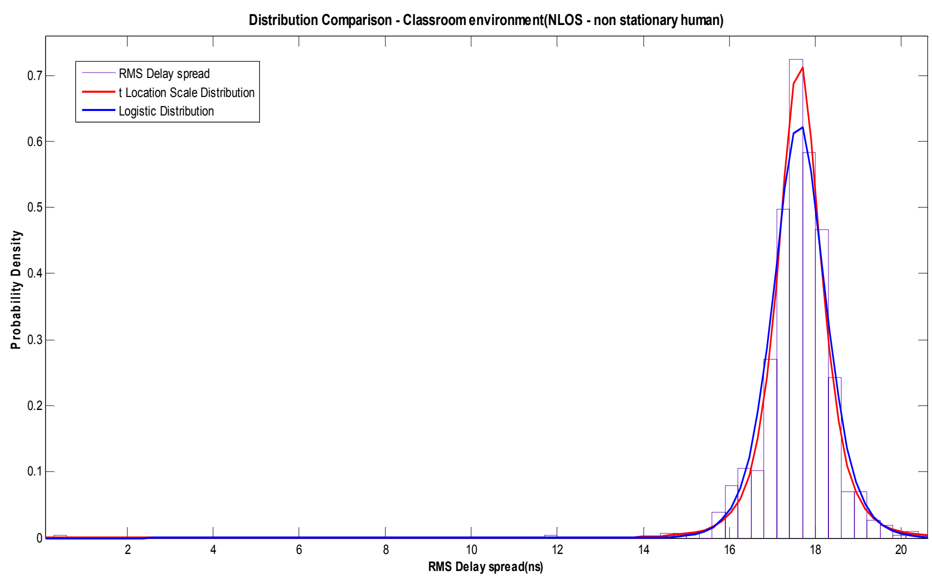

Figure 5-29 Distribution fitting for RMS Delay spread for Case 5

Table 5-22 Comparison between Distributions for case 5

Distribution Type	T Location Scale	Logistic
Log Likelihood	-1082.37	-1121.36
Mean	17.6334	17.6238
Variance	0.648173	0.521714

Table 5-23 Distribution parameters for t Location Scale Distribution (case 5)

	Parameter Estimate	Standard Error
Mu	17.6334	0.0195364
Sigma	0.515482	0.021272
Nu	3.38957	0.401147

Table 5-24 Estimated covariance of parameter estimates t Location scale distribution (case 5)

	Mu	Sigma	Nu
Mu	0.000381671	-2.02694e-05	-0.000410135
Sigma	-2.02694e-05	0.000452499	0.00571915
Nu	-0.000410135	0.00571915	0.160919

Table 5-25 Distribution parameters for LOGISTIC Distribution (case 5)

	Parameter Estimate	Standard Error
Mu	17.6238	0.0212694
Sigma	0.398224	0.0106306

Table 5-26 Estimated covariance of parameter estimates of LOGISTIC Distribution (case 5)

	Mu	Sigma
Mu	0.000452385	-3.44878e-06
Sigma	-3.44878e-06	0.000113009

5.2.6 Case 6: Transmitter and Receiver at different heights (LOS)

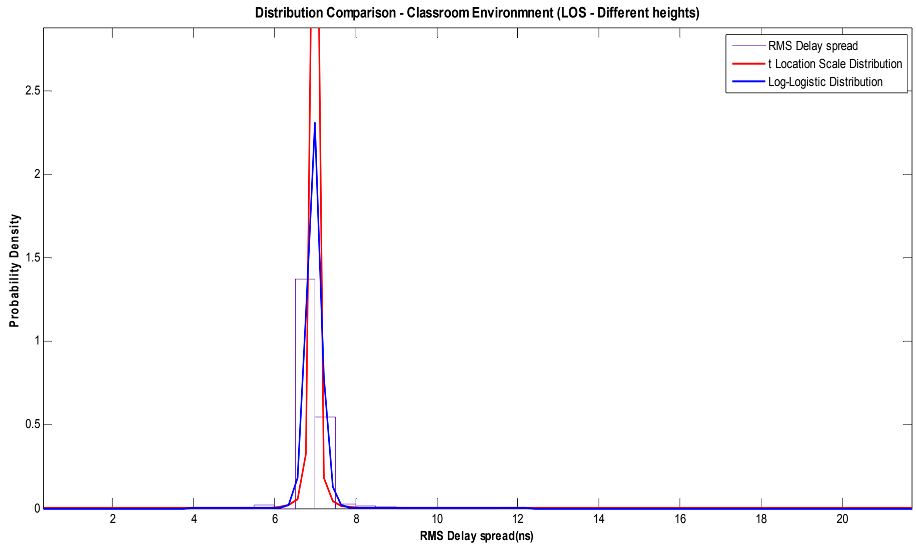

Figure 5-30 Distribution Fitting of RMS Delay spread (Case 6)

Table 5-27 Comparison between Distributions for case 6

Distribution Type	T Location Scale	Log-Logistic
Log Likelihood	917.236	-1.33586
Mean	6.96924	6.97395
Variance	Inf	0.0371545

Table 5-28 Distribution parameters for t Location Scale Distribution (case 6)

	Parameter Estimate	Standard Error
Mu	6.96924	0.00198309
Sigma	0.0445998	0.00191636
Nu	1.393	0.0829803

Table 5-29 Estimated covariance of parameter estimates t Location scale distribution

(case 6)

	Mu	Sigma	Nu
Mu	3.93266e-06	-3.6495e-07	-1.38984e-05
Sigma	-3.6495e-07	3.67242e-06	7.58744e-05
Nu	-1.38984e-05	7.58744e-05	0.00688572

Table 5-30 Distribution parameters for LOG- LOGISTIC Distribution (case 6)

	Parameter Estimate	Standard Error
Mu	1.9418	0.00072192
Sigma	0.0152314	0.00044694

Table 5-31 Estimated covariance of parameter estimates of LOG- LOGISTIC Distribution (case 6)

	Mu	Sigma
Mu	5.21169e-07	8.52452e-09
Sigma	8.52452e-09	1.99755e-07

Table 5-32 Comparison table for different distribution fits for RMS Delay spread - all cases

SL no.	**TYPE OF ENVIRONMENT**	**1ST BEST FIT**	**2ND BEST FIT**
1.	Classroom environment (TX & RX LOS – horizontal direction)	GEV	Extreme value
2.	Classroom environment (TX & RX LOS – vertical direction)	T location-scale	Logistic
3.	Classroom environment (wooden board obstruction – NLOS)	T location-scale	Logistic
4.	Classroom environment (stationary Human obstruction – NLOS)	T location-scale	Logistic
5	Classroom environment (non-stationary Human obstruction – NLOS)	T location-scale	Logistic
6.	Classroom environment (TX & RX at different heights – LOS)	T location-scale	Log – logistic

5.3 Large Scale Parameters Analysis

5.3.1 Case 1: Transmitter fixed / Receiver moving away horizontally (LOS - Last row)

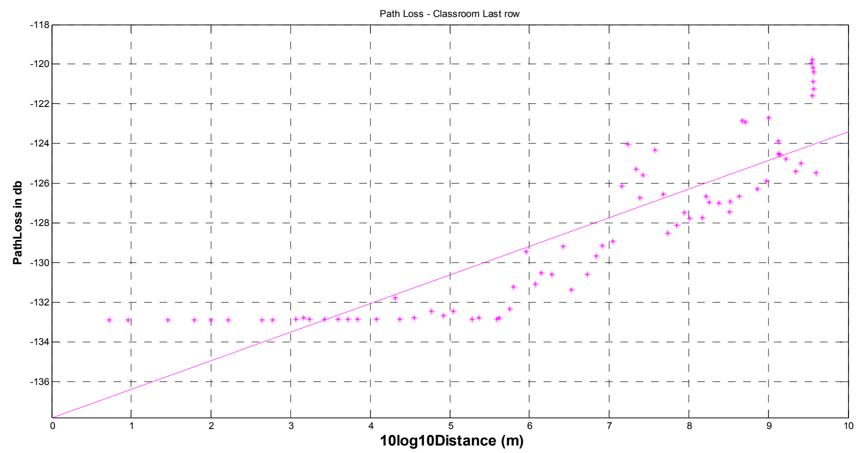

Figure 5-31 Path Loss vs. Distance (Case 1)

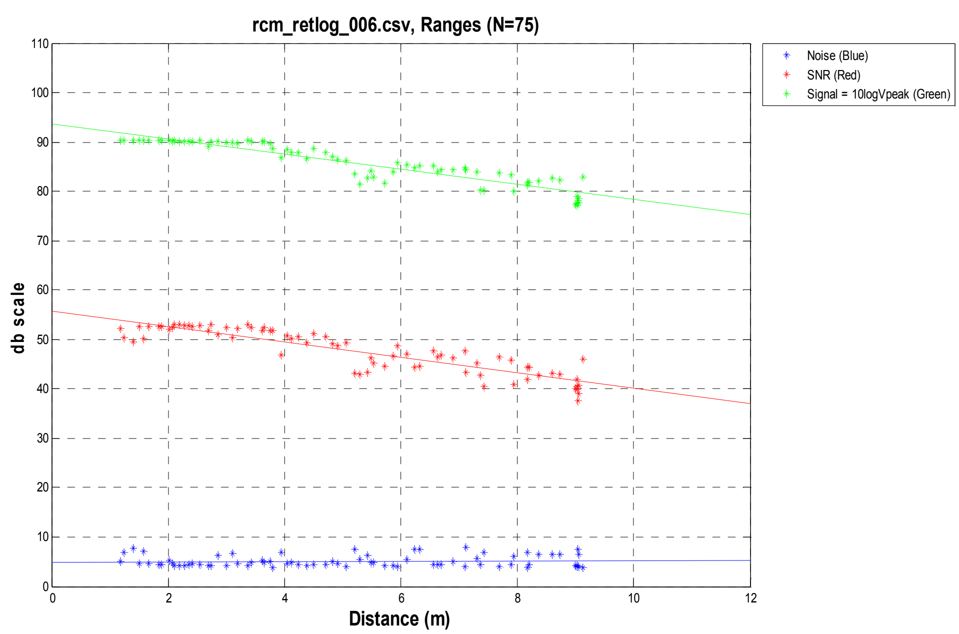

Figure 5-32 SNR, Signal Strength & Noise (dB) vs. Distance (m) - Case 1

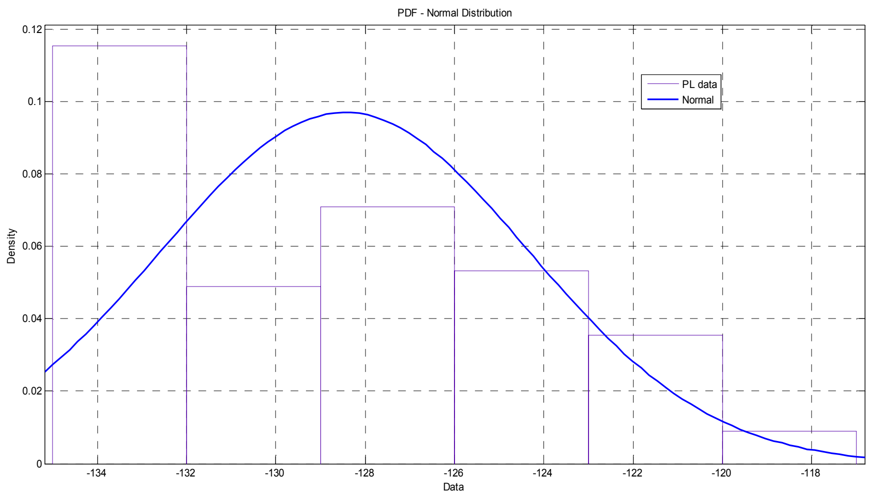

Figure 5-33 Probability Distribution Fit – Case 1

Table 5-33 Normal Distribution parameters – Case 1

Log likelihood	-212.381
Mean	-128.457
Variance	17.0977

Table 5-34 Distribution parameters – Normal Distribution (case 1)

Parameter	Estimate	Standard Err.
mu	-128.457	0.477461
sigma	4.13494	0.341044

Table 5-35 Estimated covariance of parameter estimates: Normal (case 1)

	Mu	Sigma
Mu	0.227969	-9.76574e-16
Sigma	-9.76574e-16	0.116311

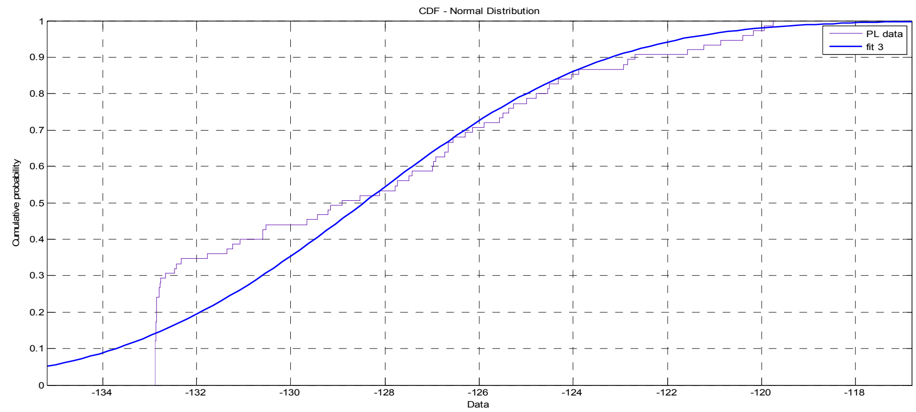

Figure 5-34 CDF of Normal Distribution – Case 1

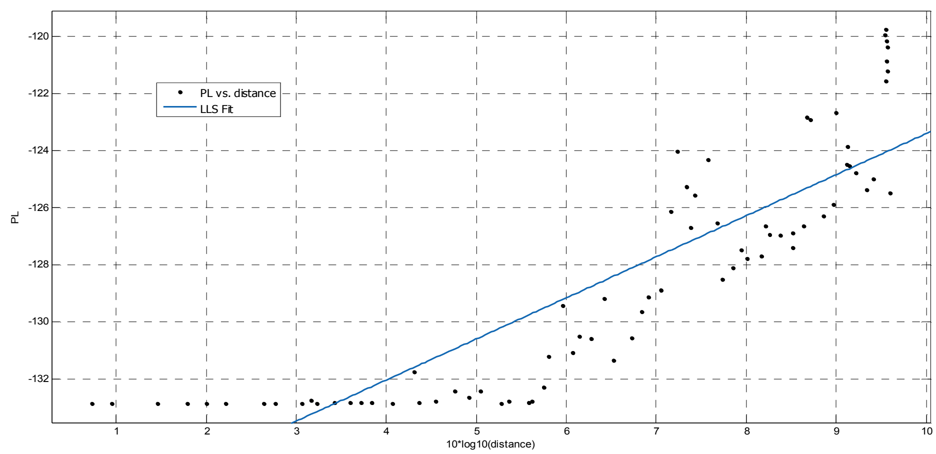

Figure 5-35 Least Linear Square Fit for Path Loss – Case 1

<u>General model:</u> Calculated from (3.5)

F (distance) = -1.328806065617482e+02+ n*distance + Y*s
Coefficients (with 95% confidence bounds):
Y = 2.388 (-2.568e+14, 2.568e+14)
n = 1.44 (1.243, 1.636)
s = -2.064 (-2.219e+14, 2.219e+14)

Goodness of fit:
SSE: 301.9
R-square: 0.7614
Adjusted R-square: 0.7548
RMSE: 2.048

5.3.2 Case 2: Transmitter Fixed / Receiver moving away vertiacally (LOS - Mid row)

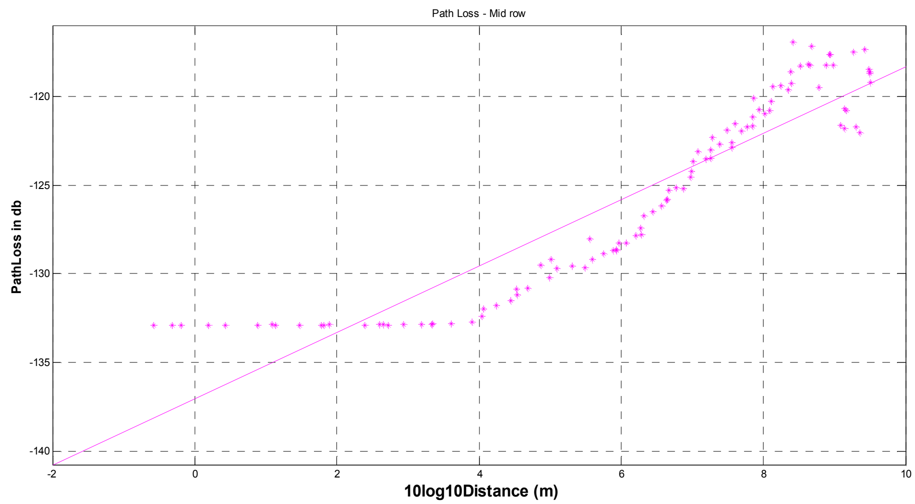

Figure 5-36 Path Loss vs. Distance – Case 2

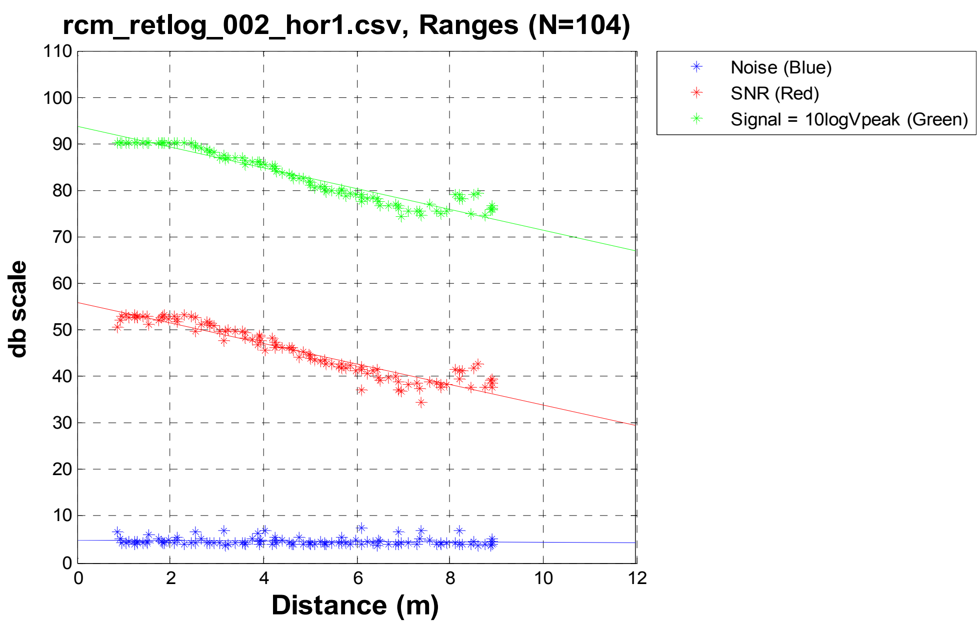

Figure 5-37 SNR, Signal Strength & Noise (dB) vs. Distance (m) – Case 2

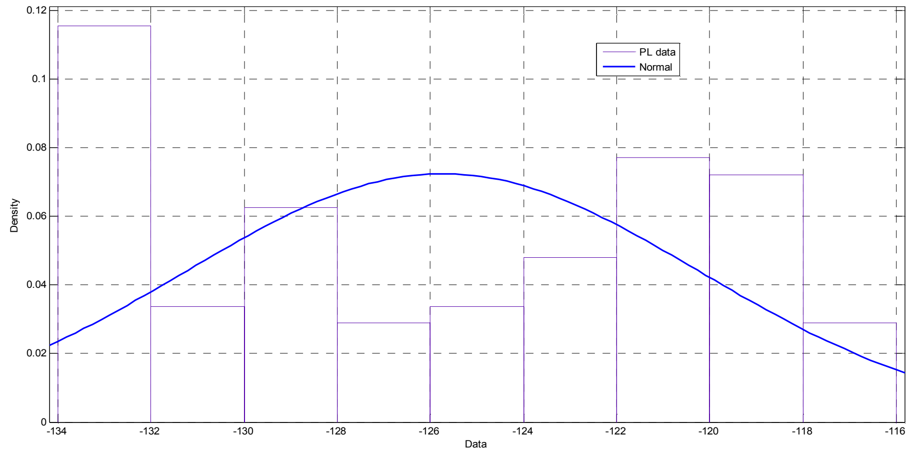

Figure 5-38 PDF for Normal Distribution – Case 2

Table 5-36 Normal Distribution parameters – Case 2

Parameters	Values
Log likelihood	-324.616
Mean	-125.736
Variance	30.3975

Table 5-37 Distribution parameters – Normal Distribution (case 2)

Parameter	Estimate	Standard Err.
Mu	-125.736	0.540633
Sigma	5.51339	0.385072

Table 5-38 Estimated covariance of parameter estimates: Normal (case 2)

	Mu	Sigma
Mu	0.292284	-1.5538e-15
Sigma	-1.5538e-15	0.148281

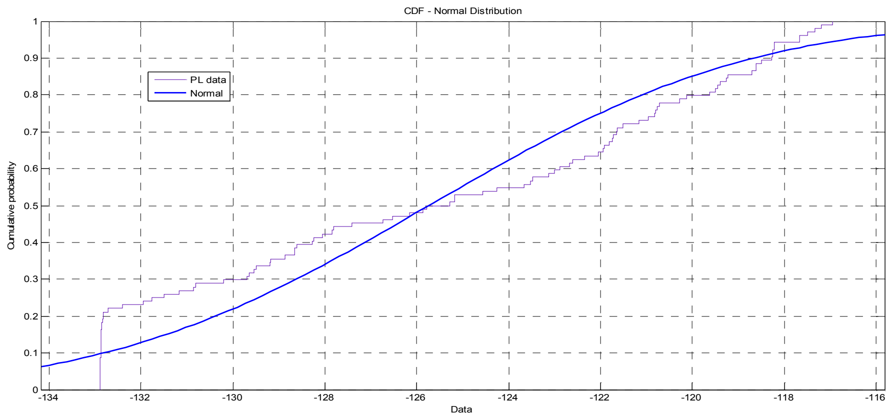

Figure 5-39 CDF of Normal Distribution

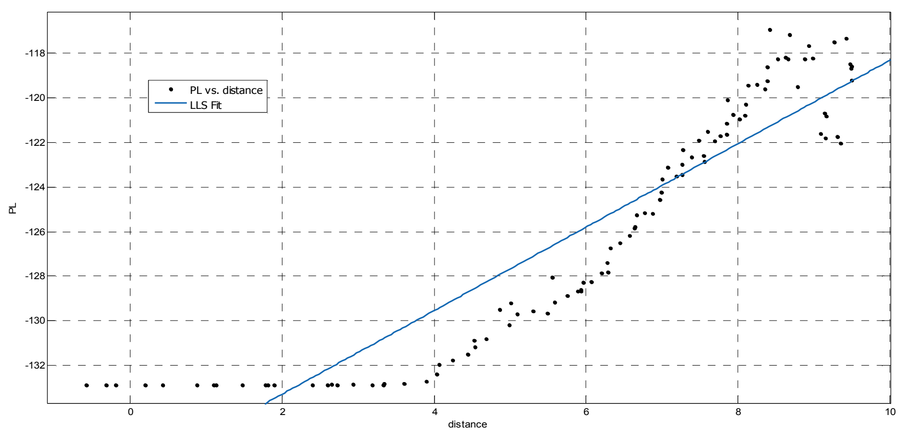

Figure 5-40 Linear Least Square Fit for Path Loss – Case 2

<u>General model:</u> Calculated from (3.5)

F (distance) = -1.328806065617482e+02+ n*distance + Y*s
Coefficients (with 95% confidence bounds):
Y = -0.2253 (-2.734e+05, 2.734e+05)
n = 1.87 (1.675, 2.064)
s = 18.36 (-2.228e+07, 2.228e+07)

Goodness of fit:
SSE: 459.8
R-square: 0.8531
Adjusted R-square: 0.8502
RMSE: 2.134

5.3.3 Case 3: Transmitter fixed / Receiver moving away in vertically (LOS)

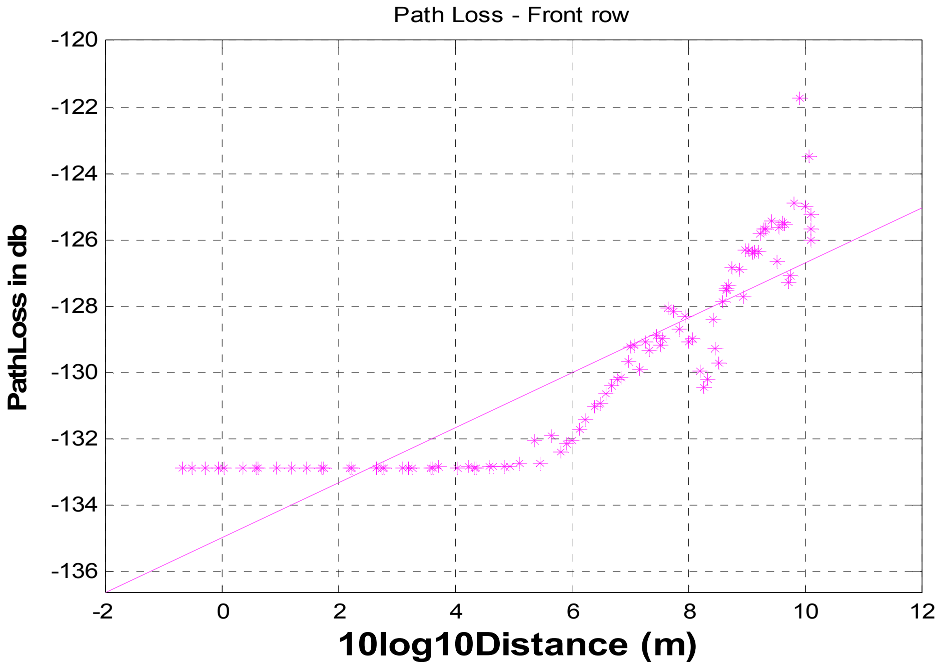

Figure 5-41 Path Loss vs. Distance – Case 3

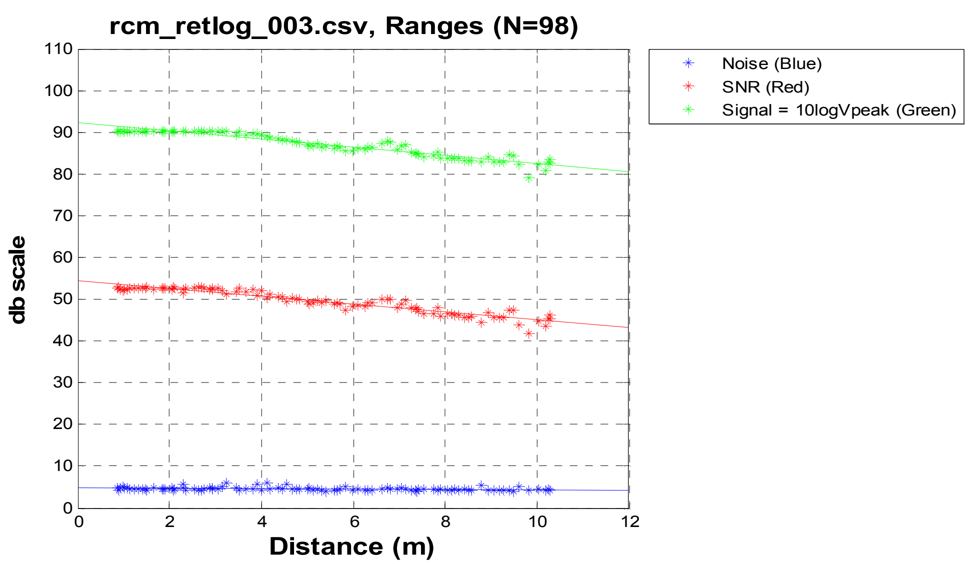

Figure 5-42 SNR, Signal Strength & Noise (dB) vs. Distance (m) – Case 3

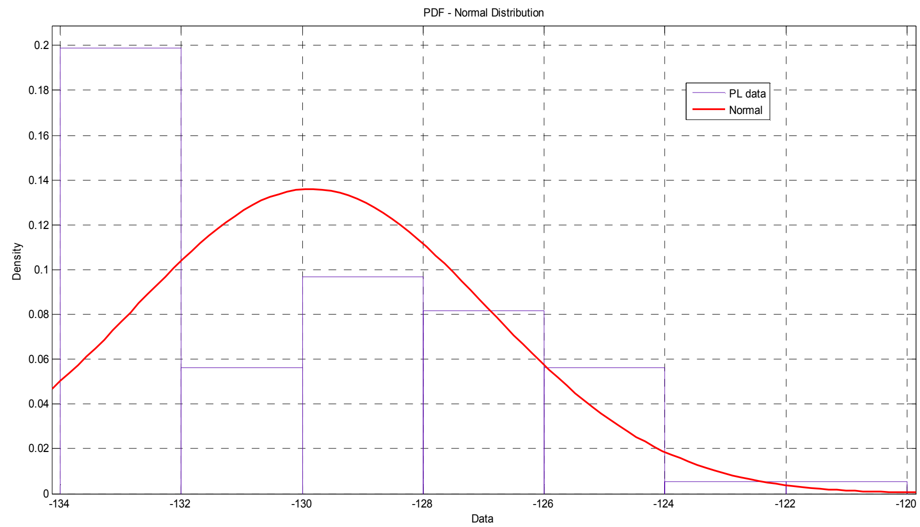

Figure 5-43 PDF of Normal Distribution

Table 5-39 Normal Distribution parameters – Case 3

Parameter	Values
Log likelihood	-244.017
Mean	-129.851
Variance	8.60441

Table 5-40 Distribution parameters – Normal Distribution (case 3)

	Estimate	Standard Err.
Mu	-129.851	0.296311
Sigma	2.93333	0.211145

Table 5-41 Estimated covariance of parameter estimates: Normal (case 3)

	Mu	Sigma
Mu	0.0878001	-2.29906e-16
Sigma	-2.29906e-16	0.0445824

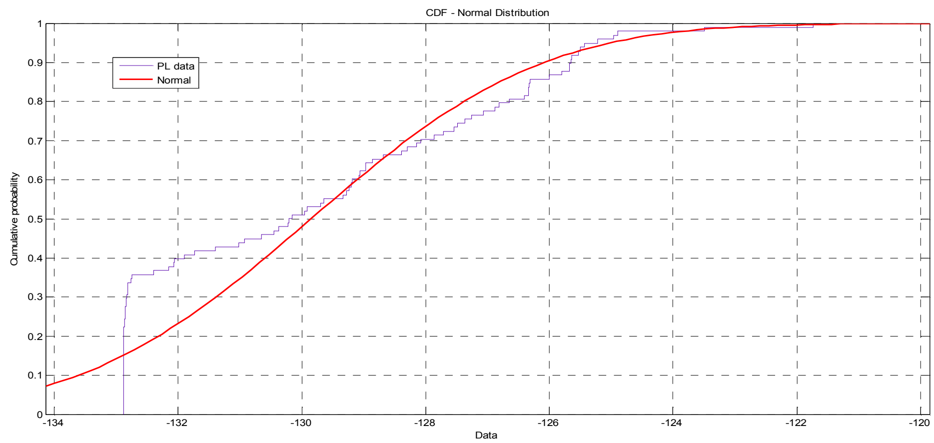

Figure 5-44 CDF of Normal Distribution – Case 3

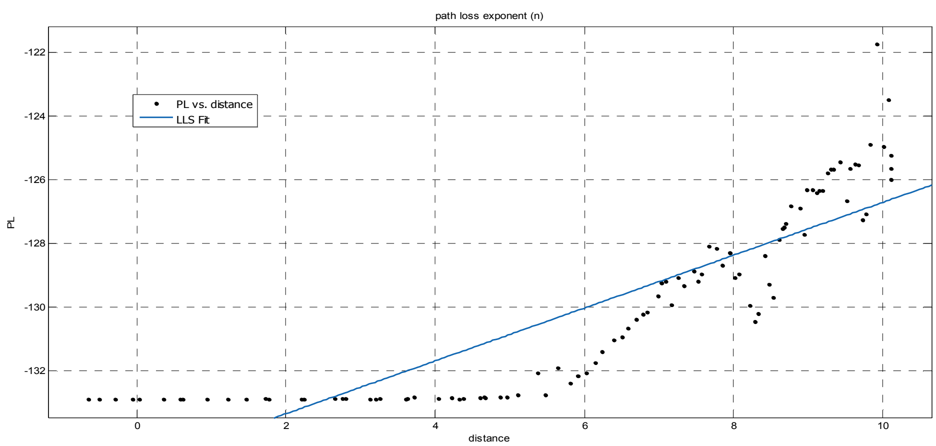

Figure 5-45 Linear Least Square Fit for Path Loss – Case 3

General model: Calculated from (3.5)

F (distance) = -1.328806065617482e+02+ n*distance + Y*s
Coefficients (with 95% confidence bounds):
Y = 1.421 (-1.555e+15, 1.555e+15)
n = 0.8291 (0.7324, 0.9257)
s = -1.487 (-1.629e+15, 1.629e+15)

Goodness of fit:
SSE: 199.7
R-square: 0.7608
Adjusted R-square: 0.7557
RMSE: 1.45

Chapter 6

CONCLUSIONS AND FUTURE WORK

6.1 Conclusion

1. Path Loss in the Classroom environment was considered for three cases out of which two cases (case 1 and case 2) reported a path loss exponent n = 1.44 and 1.87. In these cases, the LOS has a large clutter (Desks, benches and chairs), resulting in degradation of the signal over the distance covered.
2. Path Loss exponent in the Vertical movement LOS case (case 3) is reported to be n = 0.8 which is significantly less than the other two LOS cases owing to the fact that LOS path did not have any noticeable clutter like desks, benches and chairs. Hence, signal energy is consistent yielding a small slope in the path loss curve.
3. Path Loss is shown to follow Normal Distribution in all the cases.
4. The RMS delay spread values are observed to increase with the increase in distance.
5. RMS delay spread values are higher in NLOS case than in LOS environment.
6. The least RMS delay spread values were observed in the case where antennae were positioned at different heights which can explained by the fact that a good LOS existed in this case.
7. The Probability Density Functions (PDF's) of RMS delay spread for all the cases is seen to follow the T-Location Scale distribution which is consistent.
8. The mean value RMS delay spread for LOS cases varies from ~7 ns to ~14 ns depending on the clutter density in the LOS path which is a wider range as compared to 8 – 12 ns measured by IEEE model.
9. In the NLOS case, mean value varies from ~17.5ns to ~19.7ns which is high compared to 14ns – 19ns as per the IEEE model.

6.2 Future work

The analysis carried out in this thesis was performed in a classroom environment which is a limiting case. It remains to be seen what would be the effect in the case of different rooms with different infrastructure and conclude on a generalized model. This can be achieved only by extensive measurement campaigns. Also, rooms of different dimensions would yield different results which necessitate considering the effect of dimensions on the channel parameters. Also the effect of the material used for the wall can also be considered. The measurements in this thesis are limited to bi-static operation of the UWB radios. We can also explore the possibility of multi-static configuration which may lead to a better statistical approximation of channel behavior.

References

[1] Jeffrey R. Foerster, Marcus Pendergrass and Andreas F. Molisch, “A Channel Model for Ultrawideband Indoor Communication”, M. TR2003-73, November 2003

[2] FCC, Office of Engineering and Technology, ”Revision of part 15 of the commissions rules regarding ultra-wideband transmission systems”, ET Docket, no. 98-153, 2002.

[3] Joon-Yong Lee, R.A. Scholtz, ”Ranging in a dense multipath environment using an UWB radio link”, IEEE Journal on Selected Areas in Communications, vol. 20, no. 9, pp. 1677-1683, Dec. 2002.

[4] A.A. D’Amico, U. Mengali, L. Taponecco, ”Energy-based TOA estimation”, IEEE Transaction on Wireless Communications, vol. 7, no. 3, pp. 838-847, Mar. 2008.

[5] I. Guvenc, Z. Sahinoglu, ”Threshold-based TOA estimation for impulse radio UWB systems”, IEEE ICU 2005, pp. 420-425, Sept. 2005.

[6] I. Guvenc, Z. Sahinoglu, P.V. Orlik, ”TOA estimation for IR-UWB systems with different transceiver types”,IEEE Transactions on Microwave Theory and Techniques, vol. 54, no. 4, pp. 1876-1886, Jun. 2006.

[7] Joon-Yong Lee, Sungyul Yoo, ”Large error performance of UWB ranging in multipath and multiuser environments”, IEEE Transaction on Microwave Theory and Techniques, vol. 54, no. 4, pp. 1887-1895, Apr. 2006.

[8] Z. Irahhauten, H. Nikookar and G. Janssen, “An Overview of Modeling of Ultra Wide Band Indoor Channels”.

[9] Saeed S. Ghassenizadeh, Rittwik Jam Christopher W Rice, William Turin, Vahid Tarokh, “A STATISTICAL PATH LOSS MODEL FOR IN-HOME UWB CHANNELS”

[10] Time Domain Corporation, "Ranging and Communication Module (RCM), Data sheet", May 2013.

[11] Time Domain Corporation, "Monostatic Radar Module (MRM), Data sheet", May 2013.

[12] Time Domain Corporation, "Channel Analysis Tool(CAT) guide, Data sheet", March 2013.

[10] Maria-Gabriella Di Benedetto – Guerino Giancola, "Understanding Ultra Wideband – Radio Fundamentals", Pearson Education, Inc., 2004

[11] Huseyin Arslan, Zhi Ning Chen, Maria-Gabriella Di Benedetto, "Ultra wide band communications", John Wiley & Sons Inc, 2006

[12] Hashemi.H, "The indoor Radio propagation channel", Proceedings of the IEEE, Volume:81, Issue 7 (July 1993a), 943-968

[13] S. S. Ghassemzadeh, R. Jana, C. Rice, W. Turin, and V. Tarokh, "Measurement and modeling of an ultra-wide bandwidth indoor channel," IEEE Trans. Commun., vol. 52, no. 10, pp. 1786–1796, October 2004.

[14] C.-C. Chong, Y. Kim, and S.-S. Lee, "Statistical characterization of the UWB propagation channel in various types of high-rise apartments," in Proc. IEEE Wireless Communications Networking Conf. (WCNC05), New Orleans, LA, March 2005, pp. 944–949.

[15] C.-C. Chong, Y. Kim, S. K. Yong, and S.-S. Lee, "Statistical characterization of the UWB propagation channel in indoor residential environment," Wireless Commun. Mobile Comput., (Special Issue on UWBCommunications), August 2005, vol. 5, no. 5, pp. 503 512.

[16] A. F. Molisch, K. Balakrishnan, D. Cassioli, C.-C. Chong, S. Emami, A. Fort, J. Karedal, J. Kunisch, H. Schantz, and K. Siwiak, "A comprehensive model for ultrawideband propagation channels," in Proc. IEEE Global Telecommunications Conf. (GLOBECOM05),St. Louis, MO, December 2005, pp. 3648–3653.

[17] A. F. Molisch, B. Kannan, C.-C. Chong, S. Emami, A. Fort, J. Karedal, J. Kunisch, H. Schantz, U. Schuster and K. Siwiak, “IEEE 802.15.4a channel model—final report,” IEEE 802.15-04-0662-00-004a, November 2004.

[18] A. A. M. Saleh and R. A. Valenzuela, “A statistical model for indoor multipath propagation,” IEEE J. Select. Areas Commun., vol. 5, no. 2, pp. 128–137, February 1987.

[19] Yingzhi Chen, “Experimental Characterization of an Ultra-Wideband Indoor Wireless Channel”, Thesis report.

[20] Ashith Kuamar,”Experimental study of through the wall human being detection using UWB radar”, Thesis report.

Biographical Information

Shruthishree Bangalore Krishnamurthy was born in Bangalore, India in 1989. She completed her Bachelor's in Telecommunications Engineering from the Visvesvaraya Technological University, India in 2011.

She worked at Infosys Technologies Ltd, India as a Software Engineer for two years prior to joining the University of Texas at Arlington, Texas to pursue her Masters in Electrical Engineering. Shruthishree is currently working as a Modem System Test Engineer on-site at Qualcomm Inc. Her research interests lies in various aspects of Wireless Communications and Embedded systems.